

การพัฒนาวิธีตรวจวัดไฮโมซิสเทอินโดยใช้อิเล็กโทรเคมีลูมิเนสเซนซ์ของควอนตัมดอต

นางสาวตริยาภรณ์ กิตติสารกุล

วิทยานิพนธ์นี้เป็นส่วนหนึ่งของการศึกษาตามหลักสูตรปริญญาวิทยาศาสตรมหาบัณฑิต

สาขาวิชาเคมี ภาควิชาเคมี

คณะวิทยาศาสตร์ จุฬาลงกรณ์มหาวิทยาลัย

ปีการศึกษา 2555

ลิขสิทธิ์ของจุฬาลงกรณ์มหาวิทยาลัย
บทคัดย่อและแฟ้มข้อมูลฉบับเต็มของวิทยานิพนธ์ตั้งแต่ปีการศึกษา 2554 ที่ให้บริการในคลังปัญญาจุฬาฯ (CUIR)

เป็นแฟ้มข้อมูลของนิสิตเจ้าของวิทยานิพนธ์ที่ส่งผ่านทางบัณฑิตวิทยาลัย

The abstract and full text of theses from the academic year 2011 in Chulalongkorn University Intellectual Repository (CUIR) are the thesis authors' files submitted through the Graduate School.

METHOD DEVELOPMENT FOR DETERMINATION OF HOMOCYSTEINE
BY ELECTROCHEMILUMINESCENCE OF QUANTUM DOTS

Miss Triyaporn Kittisarakul

A Thesis Submitted in Partial Fulfillment of the Requirements
for the Degree of Master of Science Program in Chemistry

Department of Chemistry

Faculty of Science

Chulalongkorn University

Academic Year 2012

Copyright of Chulalongkorn University

Thesis Title METHOD DEVELOPMENT FOR DETERMINATION
OF HOMOCYSTEINE BY
ELECTROCHEMILUMINESCENCE OF QUANTUM
DOTS

By Miss Triyaporn Kittisarakul

Field of Study Chemistry

Thesis Advisor Assistant Professor Suchada Chuanuwatanakul, Ph.D.

Thesis Co-advisor Numpon Insin, Ph.D.

Accepted by the Faculty of Science, Chulalongkorn University in Partial
Fulfillment of the Requirements for the Master's Degree

.....Dean of the Faculty of Science
(Professor Supot Hannongbua, Dr. rer. nat.)

THESIS COMMITTEE

.....Chairman
(Assistant Professor Warinthorn Chavasiri, Ph.D.)

.....Thesis Advisor
(Assistant Professor Suchada Chuanuwatanakul, Ph.D.)

.....Thesis Co-advisor
(Numpon Insin, Ph.D.)

.....Examiner
(Professor Orawon Chailapakul, Ph.D.)

.....External Examiner
(Kulwadee Pinwattana, Ph.D.)

ตริยาภรณ์ กิตติสารกุล : การพัฒนาวิธีตรวจวัดโฮโมซิสเทอีนโดยใช้อิเล็กโทรเคมีลูมิเนสเซนซ์ของควอนตัมดอต. (METHOD DEVELOPMENT FOR DETERMINATION OF HOMOCYSTEINE BY ELECTROCHEMILUMINESCENCE OF QUANTUM DOTS) อ.ที่ปรึกษาวิทยานิพนธ์หลัก : ผศ. ดร. สุชาติ จุจนวัฒน์กุล, อ.ที่ปรึกษาวิทยานิพนธ์ร่วม : อ.ดร.นำพล อินสิน, 79 หน้า.

ในงานวิจัยนี้ได้พัฒนาวิธีวิเคราะห์ใหม่บนพื้นฐานของอิเล็กโทรเคมีลูมิเนสเซนซ์ของแคดเมียมเทลลูไรด์ควอนตัมดอตโดยใช้ขั้วไฟฟ้าท่อนาโนคาร์บอนพิมพ์สกรีน ซึ่งพบว่าขั้วไฟฟ้าท่อนาโนคาร์บอนพิมพ์สกรีนสามารถเพิ่มความเข้มของอิเล็กโทรเคมีลูมิเนสเซนซ์ของแคดเมียมเทลลูไรด์ควอนตัมดอตที่กระจายตัวในน้ำได้อย่างดีเยี่ยม ดังนั้นขั้วไฟฟ้าท่อนาโนคาร์บอนพิมพ์สกรีนเป็นขั้วไฟฟ้าที่ดีที่จะนำมาประยุกต์ในงานทางอิเล็กโทรเคมีลูมิเนสเซนซ์ของควอนตัมดอต ได้สังเคราะห์แคดเมียมเทลลูไรด์ควอนตัมดอตที่จับด้วยกรดไทโอไกลโคลิกเพื่อใช้ในอิเล็กโทรเคมีลูมิเนสเซนซ์ที่ใช้ขั้วไฟฟ้าท่อนาโนคาร์บอนพิมพ์สกรีน และหาลักษณะเฉพาะโดยใช้ยูวี-วิสิเบิลสเปกโทรสโกปี โฟโตลูมิเนสเซนซ์สเปกโทรสโกปี จุลทรรศน์ศาสตร์อิเล็กตรอนชนิดส่องผ่านและอินฟราเรดสเปกโทรสโกปี จากการหาลักษณะเฉพาะพบว่าขนาดอนุภาคเฉลี่ยของแคดเมียมเทลลูไรด์ควอนตัมดอตที่จับด้วยกรดไทโอไกลโคลิกมีค่าประมาณ 2.53 นาโนเมตร ซึ่งใกล้เคียงกับเส้นผ่านศูนย์กลาง 2.47 นาโนเมตรที่ได้จากการคำนวณโดยใช้ยูวี-วิสิเบิลแอบซอร์บชันสเปกตรัมของควอนตัมดอต นอกจากนี้พบว่าความเข้มข้นของแคดเมียมเทลลูไรด์ควอนตัมดอตที่จับด้วยกรดไทโอไกลโคลิกที่สังเคราะห์ขึ้นคือ 7.39×10^{-3} โมลาร์ ได้ศึกษาปัจจัยที่มีอิทธิพลต่อความเข้มของอิเล็กโทรเคมีลูมิเนสเซนซ์เพื่อใช้ตรวจวัดโฮโมซิสเทอีนโดยใช้ผลการลดลงของอิเล็กโทรเคมีลูมิเนสเซนซ์ของแคดเมียมเทลลูไรด์ควอนตัมดอต ภายใต้ภาวะที่เหมาะสม พบว่าความเข้มของอิเล็กโทรเคมีลูมิเนสเซนซ์มีความสัมพันธ์เชิงเส้นตรงกับความเข้มข้นของโฮโมซิสเทอีนในช่วง 5 ถึง 35 ไมโครโมลาร์โดยมีขีดจำกัดต่ำสุดของการตรวจวัดเท่ากับ 0.011 ไมโครโมลาร์ วิธีที่เสนอนี้ประสบความสำเร็จในการประยุกต์ใช้ตรวจวัดปริมาณโฮโมซิสเทอีนในตัวอย่างปัสสาวะมนุษย์และปัสสาวะสังเคราะห์

ภาควิชา.....เคมี.....	ลายมือชื่อนิสิต
สาขาวิชา.....เคมี.....	ลายมือชื่อ อ.ที่ปรึกษาวิทยานิพนธ์หลัก
ปีการศึกษา.....2555.....	ลายมือชื่อ อ.ที่ปรึกษาวิทยานิพนธ์ร่วม

5372403823 : MAJOR CHEMISTRY

KEYWORDS : ELECTROCHEMILUMINESCENCE / TGA-CAPPED CdTe QUANTUM DOTS / HOMOCYSTEINE / CARBON NANOTUBE-MODIFIED SCREEN PRINTED CARBON ELECTRODE

TRIYAPORN KITTISARAKUL : METHOD DEVELOPMENT FOR DETERMINATION OF HOMOCYSTEINE BY ELECTROCHEMILUMINESCENCE OF QUANTUM DOTS. ADVISOR: ASST. PROF. SUCHADA CHUANUWATANAKUL, Ph.D., CO-ADVISOR : NUMPON INSIN, Ph.D., 79 pp.

In this research, a novel analytical method based on electrochemiluminescence (ECL) of CdTe quantum dots (QDs) using carbon nanotube (CNT)-modified screen-printed carbon electrodes (SPCNTes) was developed. It was found that the SPCNTes could greatly enhance the ECL intensity of CdTe QDs dispersed in aqueous solution. Thus, SPCNTes would have a great merit to expand the application of QD ECL. The thioglycolic acid (TGA)-capped CdTe QDs used in ECL procedure based on the SPCNTes were synthesized and characterized by UV-visible spectroscopy, photoluminescence spectroscopy, transmission electron microscopy, and infrared spectroscopy. From the characterizations, the average size of TGA-capped CdTe QDs was approximately 2.53 nm, which considered close to the diameter of 2.47 nm resulting from the calculations using UV-visible absorption spectra of the QDs. Moreover, the concentration of synthesized TGA-CdTe QDs was found to be 7.39×10^{-3} M. Influences of some factors on the ECL intensity were investigated to determine homocysteine (Hcy) based on the quenching effect of CdTe QDs ECL. Under the optimal conditions, the ECL intensity has a linear relationship with the concentration of Hcy in the range of 5 to 35 μ M with the limit of detection of 0.011 μ M. This proposed method was successfully applied to determine Hcy in human urine and artificial urine samples.

Department :	Chemistry.....	Student's Signature
Field of Study :	Chemistry.....	Advisor's Signature
Academic Year :	2012.....	Co-advisor's Signature.....

ACKNOWLEDGEMENTS

First of all I would like to heartily grateful my advisor, Assistant Professor Dr. Suchada Chuanuwatanakul and my co-advisor, Dr. Numpon Insin, for helpful advice, kind encouragement, and excellent support throughout my Master's Degree study at Chulalongkorn University. I am also cordially thankful to Professor Dr. Orawon Chailapakul, for her kind advice and encouragement.

Additionally, I would like to thank my thesis examination committee, Assistant Professor Dr. Warinthorn Chavasiri and Dr. Kulwadee Pinwattana for their encouragement, insightful comments, and excellent guidance in my thesis.

Special thanks are extended to Dr. Sakchai Satienperakul, Department of Chemistry, Faculty of Science, Maejo University for his advice and providing the PMT instrument for this research.

Moreover, I would like to express my thanks to Mr. Sudkate Chaiyo and Mr. Poomrat Rattanasat, who gave me the advice, valuable helpful and sincere encouragement. My sincere appreciation is also extended to the member of electrochemical group at Chulalongkorn University for their help and friendship.

Of course, this project would not have been possible without the financially supported by 90th Anniversary of Chulalongkorn University Fund (Ratchadaphiseksomphot Endowment Fund) and the National Research University Project of CHE.

Finally, I would like to express my sincerest gratitude and deepest appreciation to my beloved family and especially my affectionate grandparents, for their helpfulness, financial support, and encouragement throughout my education and my life.

CONTENTS

	Page
ABSTRACT IN THAI	iv
ABSTRACT IN ENGLISH	v
ACKNOWLEDGEMENTS	vi
CONTENTS	vii
LIST OF TABLES	xi
LIST OF FIGURES	xii
LIST OF ABBREVIATIONS	xiv
CHAPTER I INTRODUCTION	1
1.1 Introduction	1
1.2 Objectives of the research	3
CHAPTER II THEORY AND LITERATURE SURVEY	4
2.1 Quantum Dots (QDs)	4
2.1.1 Optical properties of QDs	4
2.1.2 Synthesis of QDs	6
2.1.3 Applications of QDs	7
2.2 Electrogenenerated Chemiluminescence (ECL)	8
2.2.1 Annihilation Pathway	9
2.2.2 Co-reactant Pathway	10
2.2.3 Quenching	11
2.3 Electrochemical method	12
2.3.1 Cyclic voltammetry	14
2.4 Working electrode	16
2.4.1 Screen printed carbon electrodes	17
2.5 Carbon nanotubes	17
2.5.1 Single-wall carbon nanotubes (SWCNTs)	17
2.5.2 Multi-wall carbon nanotubes (MWCNTs)	18
2.5.3 Properties of carbon nanotubes	18

	Page
2.6 Thiol compounds.....	20
2.6.1 Homocysteine.....	21
2.7 Literature surveys.....	23
2.7.1 Conventional methods for Hcy detection.....	23
2.7.2 Electrogenerated Chemiluminescence (ECL) with carbon nanotube modified electrode.....	25
CHAPTER III EXPERIMENTAL.....	28
3.1 Instruments and equipments.....	28
3.1.1 Preparation of CdTe quantum dots.....	28
3.1.2 Characterization of CdTe quantum dots.....	29
3.1.3 Fabrication of carbon nanotubes-modified screen-printed carbon electrodes (SPCNTes).....	29
3.1.4 Electrochemiluminescence of CdTe quantum dots sensor based on the SPCNTes for determination of homocysteine (Hcy).....	30
3.2 Chemicals.....	31
3.2.1 Preparation of CdTe quantum dots.....	31
3.2.2 Fabrication of carbon nanotubes-modified screen-printed carbon electrodes (SPCNTes).....	31
3.2.3 Electrochemiluminescence of CdTe quantum dots sensor based on the SPCNTes for determination of homocysteine (Hcy)....	32
3.3 Chemical preparations.....	34
3.3.1 Preparation of CdTe quantum dots.....	34
3.3.2 Preparation of stock standard solution for determination of Hcy using CdTe QDs ECL sensor.....	34
3.4 Preparation of CdTe quantum dots.....	35
3.5 Characterization of CdTe quantum dots.....	36
3.6 Fabrication of carbon nanotubes-modified screen-printed carbon electrodes (SPCNTes).....	36

	Page
3.7 Electrogenerated chemiluminescence of CdTe quantum dots (CdTe QDs ECL) sensor based on the SPCNTEs for determination of homocysteine (Hcy).....	38
3.8 Optimization of CdTe QDs ECL conditions.....	39
3.8.1 The effect of potential.....	39
3.8.2 The effect of scan rate.....	39
3.8.3 The effect of step potential.....	39
3.8.4 The effect of concentration of CdTe QDs.....	39
3.8.5 The effect of concentration of K ₂ S ₂ O ₈ co-reactant.....	40
3.8.6 The effect of PBS pH.....	40
3.9 Reproducibility and stability study.....	40
3.10 The analytical performance.....	40
3.10.1 Linearity.....	40
3.10.2 Limit of detection (LOD) and Limit of quantification (LOQ).....	40
3.11 Interference effect.....	41
3.12 Real sample analysis.....	41
3.12.1 Determination of homocysteine in human urine sample.....	41
3.12.2 Determination of homocysteine in artificial urine sample.....	42
3.12.3 Accuracy and precision study.....	42
CHAPTER IV RESULTS AND DISCUSSION.....	43
4.1 Preparation of TGA-capped CdTe quantum dots.....	43
4.2 Characterization of CdTe quantum dots.....	44
4.2.1 UV–Vis and PL spectroscopy.....	44
4.2.2 Transmission electron microscopy.....	45
4.2.3 Infrared spectroscopy.....	46
4.3 Fabrication of carbon nanotubes-modified screen-printed carbon electrodes (SPCNTEs).....	48
4.3.1 Electrochemical behavior of SPCNTE and bare screen-printed carbon electrodes (SPCE).....	48
4.3.2 Electrochemiluminescence behavior of SPCNTE and SPCE.....	49

	Page
4.4 Electrochemiluminescence of CdTe quantum dots (CdTe QDs ECL) Sensor based on the SPCNTEs for determination of homocysteine (Hcy)	50
4.4.1 Effect of K ₂ S ₂ O ₈ co-reactant	50
4.4.2 Determination of homocysteine based on the quenching effect	53
4.5 Optimization of CdTe QDs ECL conditions	54
4.5.1 The effect of potential	54
4.5.2 The effect of scan rate	55
4.5.3 The effect of step potential	56
4.5.4 The effect of concentration of CdTe QDs	57
4.5.5 The effect of concentration of K ₂ S ₂ O ₈ co-reactant	58
4.5.6 The effect of pH of the PBS solution	59
4.6 Reproducibility and stability study	60
4.7 The analytical performance	62
4.7.1 Linearity	62
4.7.2 Limit of detection (LOD) and Limit of quantification (LOQ) ..	63
4.8 Interference effect	64
4.9 Real sample analysis	66
CHAPTER V CONCLUSIONS	68
5.1 Conclusions	68
5.2 Future perspective	69
REFERENCES	70
APPENDICES	76
VITA	79

LIST OF TABLES

Table	Page
3.1 List of instruments and equipments for the preparation of CdTe quantum dots.....	28
3.2 List of instruments and equipments for the characterization of CdTe quantum dots.....	29
3.3 List of instruments and equipments involved in the fabrication of SPCNTEs.....	29
3.4 List of instruments and equipments involved in the CdTe QDs ECL sensor based on the SPCNTEs for determination of Hcy.....	30
3.5 List of chemicals for the preparation of CdTe quantum dots.....	31
3.6 List of chemicals for the fabrication of SPCNTEs.....	31
3.7 List of chemicals for the electrochemiluminescence of CdTe quantum dots (CdTe QDs ECL) sensor based on the SPCNTEs for determination of Hcy.....	32
3.8 Preparation of 0.1 M phosphate buffer solution (PBS).....	34
4.1 Effect of interfering on the detection of Hcy.....	66
4.2 The results of Hcy determinations in real sample of human urine and artificial urine by CdTe QDs ECL.....	67
A1 The intensity of ECL signal from CTe QDs and added Hcy in the human urine sample.....	77
A2 The intensity of ECL signal from CTe QDs and added Hcy in the artificial urine sample.....	77
B1 Accuracy considered From AOAC manual for Peer Verified Methods program, VA, NOV 1993.....	78
B2 Precision considered from AOAC manual for Peer Verified Methods program, VA, NOV 1993.....	78

LIST OF FIGURES

Figure	Page
2.1 Emission of luminescence of semiconductor quantum dots	5
2.2 The size-dependent luminescence of quantum dots. Larger QDs have narrow band gaps (red QD) comparing to small QDs (blue QD)	6
2.3 A schematic illustration of the determination of BSA-OP based on a sandwich electrochemical immunoassay using quantum dots as lables	7
2.4 The reaction sequence to generate an excited state and light emission	8
2.5 ECL by ion annihilation pathway	9
2.6 ECL by co-reactant pathway of Ru(bpy) ₃ ²⁺	11
2.7 The electrochemical waveform used in voltammetry	13
2.8 Typical reversible cyclic voltammogram with the initial sweep direction towards more negative potential	15
2.9 Schematic diagrams of single-wall carbon nanotube (SWCNT) and multi-wall carbon nanotube (MWCNT)	18
2.10 Structures of Hcy, Cys and GSH	20
2.11 Metabolism of homocysteine	22
3.1 Carbon nanotubes-modified screen-printed carbon electrodes (SPCNTes) ..	37
3.2 Schematic illustration of the screen-printing procedure of the SPCNTes	37
3.3 Schematic diagram of the Electrogenerated Chemiluminescence system	39
4.1 Schematic diagram showing the preparation of TGA-capped CdTe quantum dots	43
4.2 PL and UV–Vis absorption spectra of TGA-capped CdTe QDs	44
4.3 TEM image of TGA-capped CdTe QDs	46
4.4 IR spectra of (A) TGA and (B) TGA-capped CdTe QDs	47
4.5 CV voltammograms of TGA-capped CdTe QDs at (a) bare SPCEs and at (b) SPCNTes in 0.1 PBS (pH 8)	49
4.6 ECL-time curves of TGA-capped CdTe QDs at (a) bare SPCEs and at (b) SPCNTes in 0.1 M PBS (pH 8)	50

	Page
4.7 The mechanism of ECL of CdTe QDs on the SPCNTE.....	51
4.8 ECL-time curves of TGA-capped CdTe QDs at SPCNTEs in 0.1 M PBS (pH 8) (a) in the absence of $S_2O_8^{2-}$ and (b) in the presence of 0.005 M $S_2O_8^{2-}$	52
4.9 ECL-time curves of TGA-capped CdTe QDs at SPCNTEs in 0.1 M PBS (pH 8) containing 0.005 M $K_2S_2O_8$ in the presence of homocysteine at the concentration of 20 μ M.	54
4.10 Effect of potential on CdTe QDs ECL.....	55
4.11 Effect of scan rate on CdTe QDs ECL.....	56
4.12 Effect of step potential on CdTe QDs ECL.....	57
4.13 Effect of concentration of CdTe QDs.....	58
4.14 Effect of concentration of $K_2S_2O_8$ on CdTe QDs ECL	59
4.15 Effect of PBS pH on CdTe QDs ECL.....	60
4.16 Reproducibility and stability of SPCNTEs	61
4.17 ECL-time curves of TGA-capped CdTe QDs at SPCNTEs in 0.1 M PBS (pH 8) containing 10 mM $K_2S_2O_8$ in the presence of homocysteine at the concentration of 5, 10, 15, 20, 25, 30 and 35 μ M.....	62
4.18 Calibration curve for determination of Hcy	63
4.19 The effect of cysteine on the detection of Hcy.....	64
4.20 The effect of glutathione on the detection of Hcy.....	65

LIST OF ABBREVIATIONS

ECL	electrochemiluminescence
CdTe QDs	cadmium telluride quantum dots
CNTs	carbon nanotubes
CV	cyclic voltammetry
Cys	cysteine
GSH	glutathione
Hcy	homocysteine
IR	infrared spectroscopy
LOD	limited of detection
LOQ	limited of quantitation
MWCNTs	multi-wall carbon nanotubes
μM	micromolar
mg	milligram
mL	milliliter
SD	standard deviations
SPCE	screen printed carbon electrode

SPCNTes	carbon nanotubes-modified screen printed carbon electrodes
RSD	relative standard deviations
PBS	phosphate buffer solution
PL	photoluminescence
PMT	photomultiplier tube
PVC	polyvinyl chloride
QDs	quantum dots
TEM	transmission electron microscopy
TGA	thioglycolic acid
UV-vis	ultraviolet-visible
V	volt

CHAPTER I

INTRODUCTION

1.1 Introduction

In recent years, semiconductor nanocrystals (NCs) with excellent luminescent properties have been extensively attracted much interest due to their promising applications in many fundamental areas and technical importance [1-3]. The NCs' subclass, widely known as quantum dots (QDs), are newly emerging nanomaterials, which have considerable attention due to their variety of superior optical and electrical properties. With several advantages compared with conventional luminescence materials, QDs provide a high photoluminescence (PL) quantum yield (QY), unique optical, tuneable emission wavelength from their quantum size effect, multiplexing capabilities, and long-term photostability against photo-bleaching [4-6]. Especially, semiconductor QDs in Group II-VI including CdS, CdSe, and CdTe have been the most studied because their emission in the visible range can be simply tuned by changing their diameter and the advances in their preparation methods.

Electrochemiluminescence or electrogenerated chemiluminescence (ECL) is a sort of chemiluminescence (CL), a phenomenon that a chemiluminescence reaction is initiated and controlled by the application of an electrochemical potential. Luminophore species was generated by applying potential at the electrode undergo high-energy electron-transfer reaction to form excited states. And emission of light is produced when the excited molecule decays to the ground state [7-9]. ECL is well known as an alternative method for various analytes detections. The concept combines two techniques including luminescence and electrochemistry, which results in providing more effective selectivity. For example, the timing and spatial location of the luminescent reaction can be selectively controlled. In addition to rapidity and simplicity of this method, high sensitivity can be achieved due to its low background intensity. Consequently, ECL has been widely used in a large number of analytical chemistry in recent years [10-12]. Moreover, the number of publications related to

ECL involving quantum dots (QDs) have increased significantly due to their optical, electrical, electrochemical and luminescent properties. ECL study using QDs was begun by Bard and his coworkers [13], who firstly reported ECL coupled with the use of Si QDs in an organic solvent with various types of co-reactant. Si QDs could generate light emission during potential cycling voltammetry. Since then, the ECL analytical techniques coupled with QDs have been rapidly developed; however, the effective methods to enhance QDs ECL performance are still required for further development and applications of ECL in analytical field.

Carbon nanotubes (CNTs) have been exploited as electrode materials due to their outstanding electronic, surface area, stable chemical, and strengthening mechanical properties. CNTs-modified electrodes can exhibit excellent abilities compared with bare electrodes [14] and have been widely used in conventional electrochemistry [15] and ECL systems [16] because the CNTs can easily transfer electron between the electroactive species and the electrode. On the other hand, the screen-printed carbon electrode (SPCE) is popular due to its low cost, flexibility to design, and easy to fabricate and modify, which later inspires an interesting alternative for analytical field from the incorporation between and CNT and SPCE. Hence, according to the advantages of both CNTs-modified SPCE (SPCNTes) and QDs, we were encouraged to study the CdTe QDs of ECL using SPCNTes for the determination of homocysteine (Hcy). We expect that, by reducing the injection barrier of electrons to the QDs, the enhanced QDs ECL could be benefit for both studying of QDs ECL and accelerating the application of QDs ECL in analytical field.

Hcy, sulfur-containing amino acids, which is analyte of interest shows itself an important role in biochemistry and is a key health indicators or biomarker. In human, Hcy synthesized from methionine (Met) each day is converted to cysteine (Cys) under controlled specific enzyme condition. High levels of Hcy in body are associated with a high risk factor for Alzheimer's disease [17], osteoporosis [18], neural tube defects [19] and cardiovascular disease [20]. Thus, clinical diagnosis requires the analytical method for the determination of Hcy in biological fluid. Current methods for the determination of Hcy levels are provided with several separation methods including gas chromatography (GC), high performance liquid chromatography (HPLC), and capillary electrophoresis (CE). These separation methods are commonly coupled with

mass spectrometry (MS), electrochemical, ultraviolet-visible (UV-Vis), or fluorescent detection. However, because these methods are complicated, time-consuming, and costly. In this research, we try to overcome these problems and propose a novel strategy for Hcy determination based on the quenching effect of TGA-capped CdTe QDs ECL by using the CNTs-modified screen-printed electrodes (SPCNTEs), which are simple, rapid, sensitive, inexpensive, flexible to design, and easy to fabricate and modify. The TGA-capped CdTe QDs ECL procedure based on the SPCNTEs was successfully carried out for the real determination of Hcy levels in human urine sample.

1.2 Objectives of the research

There are three main goals for this research as follows:

1. To synthesize and characterize of TGA-capped CdTe QDs
2. To develop the method for the determination of Hcy based on the quenching effect of TGA-capped CdTe QDs ECL sensor using SPCNTEs.
3. To apply the developed method for the determination of Hcy in real samples.

CHAPTER II

THEORY AND LITERATURE SURVEY

2.1. Quantum Dots (QDs)

Quantum dots (QDs) are colloidal semiconductor nanocrystals with a typical diameter of 1-20 nm, containing as few as 100 to 100,000 atoms in each particle. As a nanomaterial with confinement in all three spatial dimensions, QDs exhibit properties that are between those of bulk semiconductors and those of discrete molecules. The most widespread QDs are the binary semiconductor compounds consisting of groups II-VI, III-V, or IV-VI, emphasizing to materials such as cadmium selenide (CdSe) [21], cadmium telluride (CdTe) [21], cadmium sulfide (CdS) [21], zinc selenide (ZnSe) [22], lead sulfide (PbS) [23], and indium phosphide (InP) [24], etc.

2.1.1. Optical properties of QDs

With a size typically between 1 and 10 nm QDs show optical, electronic and mechanical properties quite different from those exhibited by bulk materials. In bulk semiconductors the large number of atoms leads to the formation of almost continuum of energy levels. The valence band (VB), comprising the lower energy levels, is filled with electrons and separated from the empty conduction band (CB), corresponding to the higher energy levels, by a fixed energy gap. Attributed to the energy band structure of semiconductor and the nanosize, QDs exhibit prominent photoluminescence (PL) properties, which can be illustrated in Figure 2.1. As can be seen, QDs have discrete energy levels in both the valence band and the conduction band, since there are atoms with limited number in each particle. When being excited by an energy (E_{ex}) higher than the band gap energy (E_g), electrons in the valence band absorb the energy and 'jump' to the conduction band, forming short-lived electron-hole pairs (the so-called excitons). Then the electrons and holes recombine quickly, and photons are emitted with a specific energy corresponding to the band gap, which is the band edge emission. As part of the energy may be released in a non-radiative way due to the Stokes shift (ΔE), the emission energy (E_{em0}) is usually lower than the

excitation energy. When there are some trap states existing in the band gap, more possible emissions can happen with various energies (i.e., E_{em1} , E_{em2} , E_{em3} , E_{em4}), which are usually lower than the band gap emission energy (E_{em0}).

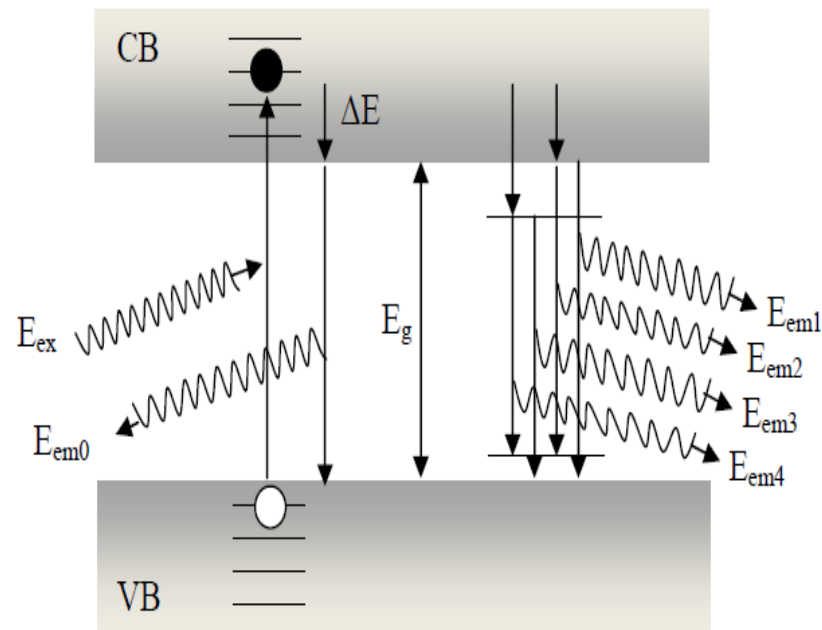


Figure 2.1 Emission of photons of semiconductor quantum dots

Similarly to the particle-in-a-box model a stronger confinement leads to a larger separation of the energy levels and therefore the band-gap of semiconductor QDs increases as size decreases resulting in the emission of light at shorter wavelengths (blue shift) (Figure 2.2). Oppositely, the band-gap decreases as more atoms are added to the nanocrystal with the lower limit of the band-gap corresponding to the bulk material. In addition, increasing the nanoparticles size leads not only to an increase in the emission wavelength (red shift) but also to a decrease in the molar extinction coefficient. Since QDs emission is size-dependent, they can be tailored in a controlled way by adjusting the synthesis conditions to assure a fluorescence emission matching virtually any wavelength of the visible region. Apart from the band-gap tunability, QDs exhibit other relevant photoluminescent properties, namely an intense and highly stable against photobleaching fluorescence, potentially high quantum yield, broad absorption and narrow, symmetric emission spectra and long excited-

state decay lifetimes. Moreover, the broad absorption bandwidth, due to the presence of multiple electronic states at higher energy levels, allows simultaneous excitation of multicolour QDs using a single light source.

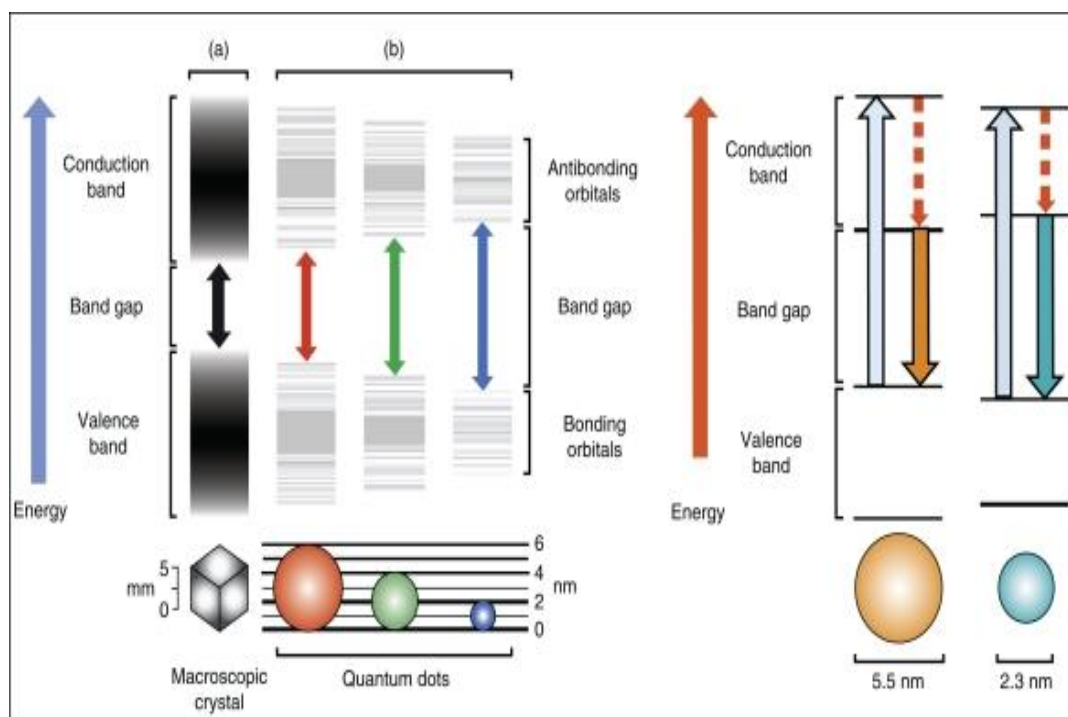


Figure 2.2 The size-dependent luminescence of quantum dots. Larger QDs (red QDs) have narrow band gaps comparing to small QDs (blue QDs) [25].

2.1.2. Synthesis of QDs

Recently, methods for synthetic colloidal QDs can be divided into two categories depending on the nature of the solvent. The solvent selection is crucial at various levels as it determines not only the nanocrystals synthesis and solubility conditions but also their chemical functionality and applicability. Wet chemistry uses low-temperature polar solvents such as water or methanol. Organometallic synthesis uses high temperature, non-polar solvents such as trioctylphosphine oxide (TOPO). Within each category, there are several variations in the exact precursors, solvents, and special additives, as well as in the temperatures and pressures required.

In alternative, numerous methods to directly synthesize water-soluble QDs were developed. These methods resort to hydrophilic capping ligands that form a thin layer at the semiconductors surface by covalent or ligand-ion electrostatic interactions. Advantageous characteristics of these methods are high simplicity and reproducibility, and also easily scaled-up for large amount production. In this regard, short-chain thiols (exhibiting as well other functional groups such as carboxylic, amino, hydroxylic, etc.) like TGA, MPA, cysteamine, have gained a noteworthy relevance as passivating agents as they provide bright QDs with a flexible surface chemistry that remain stable for years.

2.1.3. Applications of QDs

QDs have been used and presented great potentials in many applications.

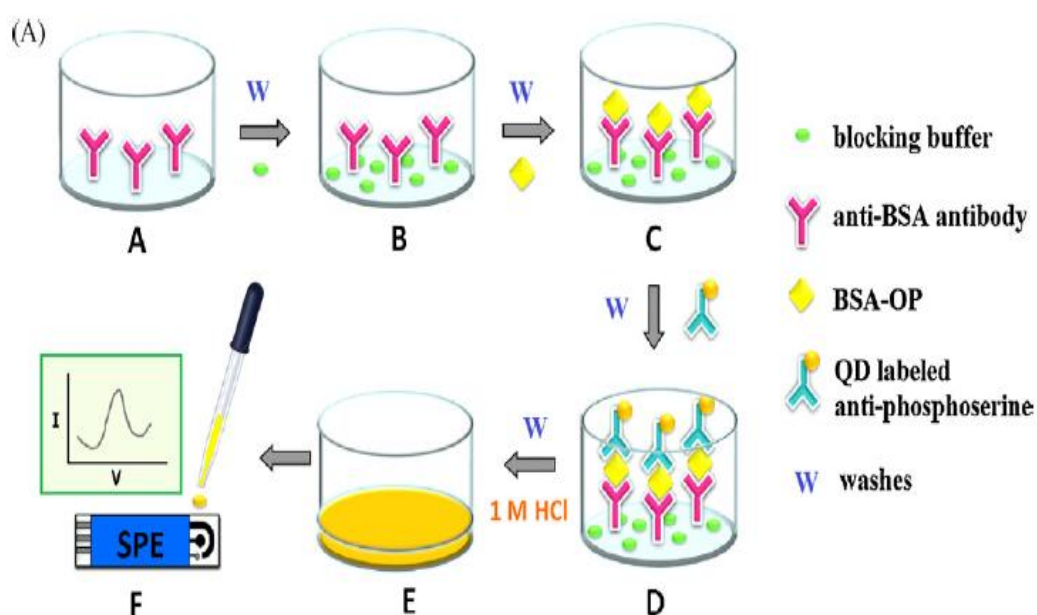


Figure 2.3 A schematic illustration of the determination of BSA-OP based on a sandwich electrochemical immunoassay using quantum dots as labels.

In electrochemical filed, the electrochemical immunosensor using CdSe/ZnS QDs labeling for the determination of phosphorylated BSA was demonstrated. The released metal ions from QDs labels were determined by electrochemical stripping analysis, as shown in Figure 2.3 [26]. The novel modified electrode constructed by immobilizing thioglycolic acid-capped CdTe QDs at a CGE with Nafion ionomer for the electrocatalysis of oxygen reduction reaction has also been displayed [27].

As it was earlier referred to, in recent years QDs have appeared as ECL chemosensor and biosensor with significant advantages regarding comparable other organic molecular. The beginning of ECL study using QDs was started by Bard and his coworkers [13], who firstly reported ECL coupled with the use of Si QDs in an organic solvent with various types of co-reactant. On quenching principle, the anodic ECL of CdTe QDs in aqueous system was reported. With catechol derivatives as model analytes, the ECL energy transfer was observed from the excited QDs to quencher, which resulted in the decrease of anodic ECL emission of QDs [29]. Based on this observation, a method for ECL detection of quencher-related analytes was proposed, and was also used for ECL analysis of L-adrenalin, tyrosine [30] and glutathione [31].

2.2. Electrochemiluminescence (ECL)

Electrochemiluminescence or electrogenerated chemiluminescence (ECL) is a phenomenon that a chemiluminescence (CL) is initiated and controlled by the application of an electrochemical potential, making luminophore species generated at the electrode undergo high-energy electron-transfer reaction to form excited states, and emission of light is then presented as shown in Figure 2.4.

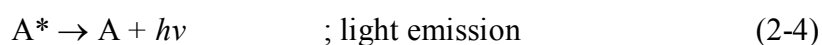
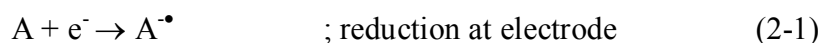


Figure 2.4 The reaction sequence to generate an excited state and light emission.

However, the difference between CL and ECL is how to control a light emission. In CL, luminescence is governed by only mixing or allowing the flow of an emitter with necessary reagents in a reaction vessel. In contrast, a light emission is controlled by turning on/off the electrode potential in ECL. As an analytical technique, ECL has some advantages over CL as following: (1) ECL has more spatial freedom than CL in that the emission spot can be controlled and manipulated by moving an electrode or varying the size/number of electrodes because ECL reaction occurs only in the diffusion layer of an electrode, (2) ECL can be more selective than CL in that the generation of excited states can be selectively controlled by varying the electrode potentials, (3) ECL is a non-destructive technique because ECL emitters are regenerated after the ECL emission. ECL is well-known as an alternative method for detection of various analytes since it combines the advantages of luminescence and electrochemical techniques providing the added selectivity. For instance, the timing and spatial location of the luminescent reaction can be selectively controlled. In addition to rapidity and simplicity of this method, high sensitivity can be achieved due to its low background intensity.

ECL can be produced through two main pathways, namely the annihilation and co-reactant pathway. In each case, two species are generated electrochemically, and those two species undergo an electron-transfer reaction to produce an emissive species.

2.2.1. Annihilation Pathway

ECL originated by ion annihilation is possible when the emitter (R) can electrochemically produce both sufficiently stable radical cation ($R^{\bullet+}$) and anion ($R^{\bullet-}$). The produced radical ions are annihilated by the oppositely charged radical ion to generate the excited state (R^*), as shown in Figure 2.5.



Figure 2.5 ECL originated by ion annihilation pathway.

These species then interact to produce both a ground state and an electronically excited state, which then relaxes by emission. Depending on the energy available in an ion annihilation (Equation 2-7), the produced R^* could be either the lowest excited singlet state species ($^1R^*$) or the triplet state species ($^3R^*$).

An advantage of the annihilation pathway is that it requires only the electrochemiluminescent species, solvent, and supporting electrolyte to generate light. However, the potential window of water is often not sufficiently wide to allow the luminophore to be both oxidized and reduced, making it necessary to use organic solvents such as acetonitrile and N,N-dimethylformamide [9].

2.2.2. Co-reactant Pathway

Co-reactant is a compound that can generate a reactive intermediate (a strong reducing or oxidizing agent) by a reaction following the electrochemical or chemical electron transfer reaction. Use of a co-reactant is useful especially when one of $R^{+\bullet}$ or R^{\bullet} is not stable enough for ECL reaction, or when the ECL solvent has so narrow potential window that $R^{+\bullet}$ or R^{\bullet} cannot be formed. In an aqueous solvent, the use of a co-reactant is very important because water has the narrow potential window, low solubility for many organic compounds, and many radical ions of organic emitters are unstable in an aqueous solvent.

The co-reactant used for ECL was oxalate ion ($C_2O_4^{2-}$). When $C_2O_4^{2-}$ is oxidized, it produces the strong reducing agent, $CO_2^{\bullet-}$, and CO_2 . For example, the aqueous solution of $Ru(bpy)_3^{2+}$ can produce ECL in the presence of $C_2O_4^{2-}$ via processes shown in Figure 2.6 [33]. In addition, aliphatic amines and peroxodisulfate ($S_2O_8^{2-}$) have been used as co-reactants.

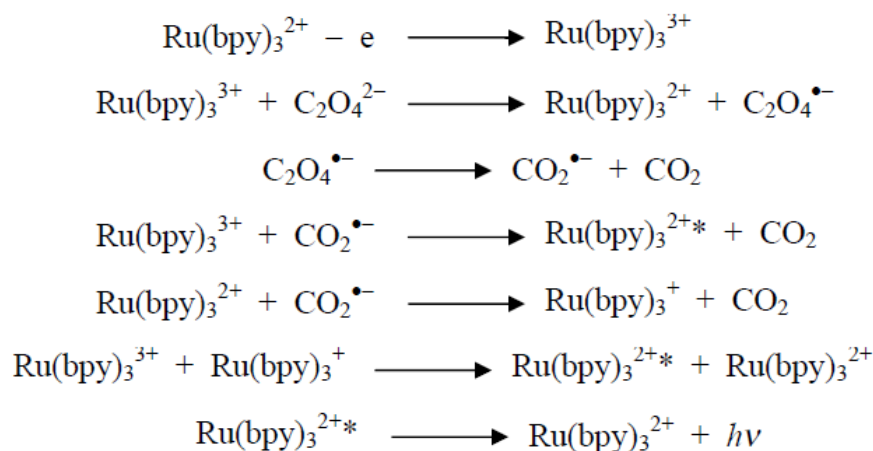
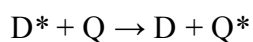


Figure 2.6 ECL originated by co-reactant pathway of Ru(bpy)_3^{2+} .

To be a good co-reactant, the following criteria should be met: (1) the co-reactant should be reasonably soluble in a solvent because the ECL intensity is generally proportional to the concentration of it, (2) the co-reactant should be easily oxidized or reduced with the ECL emitter at or near the electrode and undergo a following rapid chemical reaction to form a reactive intermediate, (3) the co-reactant and its intermediate should have inert or weak quenching effect on ECL, (4) the reactive intermediate species generated electrochemically and chemically should be stable enough for the duration of the ECL experiment, (5) the rate of a reaction between the intermediate and the radical ion of an ECL emitter must be rapid, and (6) the co-reactant itself should not produce any light emission.

2.2.3. Quenching

Quenching refers to any process which decreases the light emission intensity of a given substance. An excited state can be quenched by another molecule (a quencher, Q) to produce the ground state, i.e.



where Q^* can often decay to the ground state without emission. Quenching can occur by either energy transfer or electron transfer. Energy transfer is favored by the electronic energy of D^* being greater than that of Q^* and a large overlap of the emission band of D^* with the absorption band of Q. The energy transfer occurs by a

direct electrodynamic interaction between D^* and Q and occurs at short distances between the reactants. Electron transfer quenching occurs because the excited state is easier to be oxidized and easier to be reduced than the corresponding ground state of the same molecule, by an amount essentially equal to the excitation energy of the molecule.

2.3. Electrochemical method

Electrochemical methods are the important method for analytical chemistry which based on the monitoring of changes in an electrical signal occurring from the electrochemical reaction at an electrode surface. The typical characteristic of all voltammetric methods involves the application of a potential to an electrode in electrochemical cell. In many instances the applied potential is varied or the current is monitored over a period of time. Therefore, all voltammetric methods can be described as function of potential, current, and time, as shown in Figure 2.7. They are considered active methods because the applied potential forces a change in the concentration of an electroactive species at the electrode surface by electrochemically reducing or oxidizing it.

The analytical advantages of the several methods include excellent sensitivity with a very large useful linear concentration range for inorganic and organic species, a large number of useful solvents and electrolytes, a wide range of temperatures, rapid analysis times, and simultaneous determination of various analytes. Moreover, electrochemical methods also comprise the ability to determine kinetic and mechanistic parameters, the ability to reasonably estimate the values of unknown parameters, and the ease with which different potential wave forms can be generated.

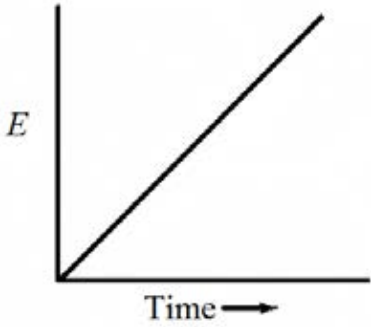
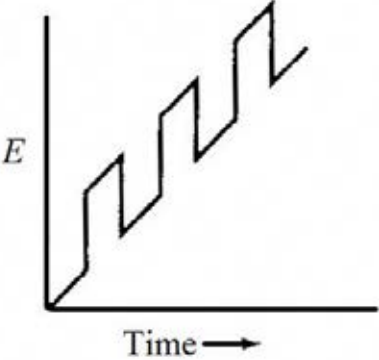
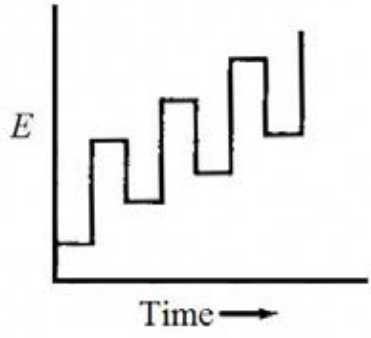
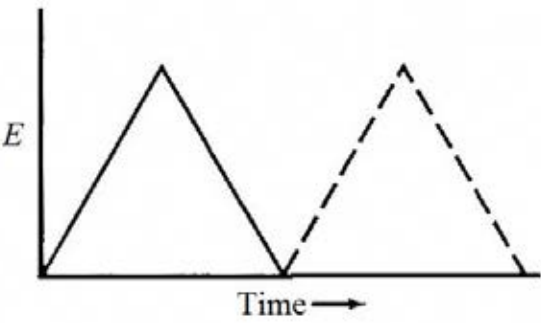
Waveform	Type of voltammetry
	Linear-scan voltammetry
	Differential voltammetry
	Square-wave voltammetry
	Cyclic voltammetry

Figure 2.7 The electrochemical waveform used in voltammetry.

In this part some electrochemical method used in this thesis including cyclic voltammetry, which is described.

2.3.1. Cyclic voltammetry

Cyclic voltammetry has become an important and widely used electroanalytical method. It is rarely used for quantitative determinations, but it is generally used for the study of redox processes to understand the reaction of intermediates, and to obtain the stability of reaction products. Cyclic voltammetry is a completed voltage scan (y axis) versus time (x axis) in forward and backward directions, as shown in Figure 2.7. For example, the initial scan could be in the negative direction to the switching potential. At that point the scan would be reversed and run in the positive direction, depending on the analysis. This method provides information about the properties and characteristics of the electrochemical process and also gives insight into any complicating side processes, for instance pre- and post-electron-transfer reactions as well as kinetic considerations.

For the period of the potential sweep, the potentiostat measures the current resulting from the applied potential. This resulting plot is called cyclic voltammogram, as shown in Figure 2.8. The voltammogram illustrates the shape of a reversible cyclic voltammogram during a single potential cycle. It is assumed that only the oxidized form (O) is present initially. Consequently, a negative-going potential scan is selected for the first half cycle, starting from a value where no reduction occurs.

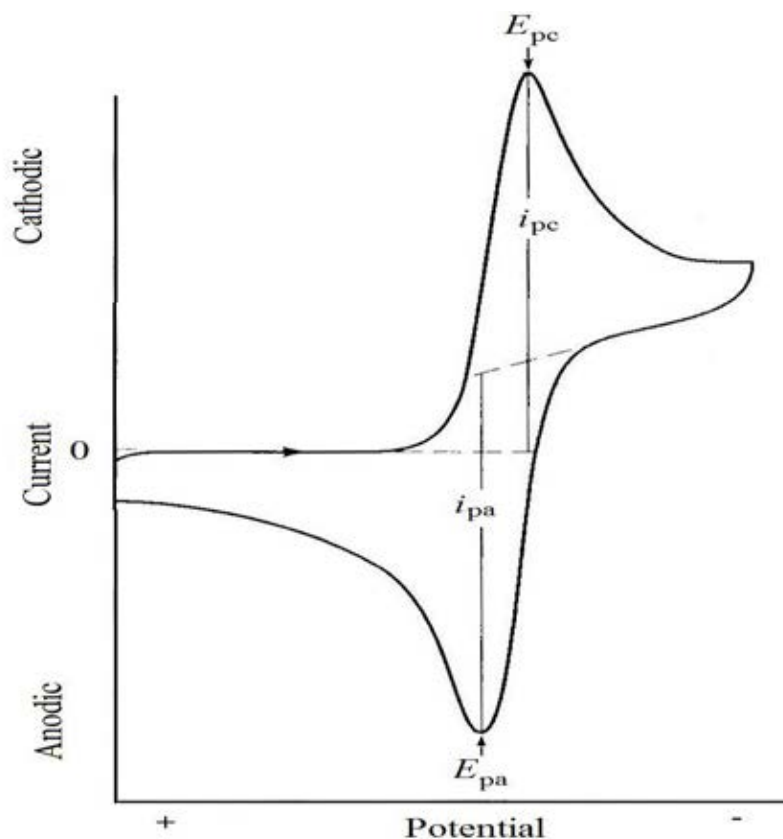


Figure 2.8 Typical reversible cyclic voltammogram with the initial sweep direction towards more negative potential.

While the applied potential approaches the characteristic E^0 for the redox process, a cathodic current begins to increase, until a peak is reached. During reverse scan, R (reduced form) molecules, which were generated in the forward half cycle and accumulated near the electrode surface, are reoxidized back to O as shown in the anodic peak results.

The voltammogram is characterized by a peak potential, E_p , at which the current reaches its maximum value and that value is called the peak current, i_p . The $i_{p,a}$ and $E_{p,a}$ are anodic peak current and anodic peak potential, respectively. The $i_{p,c}$ and $E_{p,c}$ are cathodic peak current and cathodic peak potential, respectively. The peak currents are commonly measured by extrapolating the preceding baseline current. The peak current for a reversible couple is given by the Randles-Sevcik equation:

$$i_p = (2.69 \times 10^5) n^{3/2} A C D^{1/2} \nu^{1/2} \quad \text{at } 25 \text{ }^\circ\text{C} \quad (2-9)$$

where i_p is in ampere (A), A (electrode area) is in cm^2 , D (diffusion coefficient) is in $\text{cm}^2 \text{ s}^{-1}$, C (concentration of electroactive species) is in mol cm^{-3} , and ν (scan rate) is in V s^{-1} .

The ratio of the reverse-to-forward peak currents, $i_{p,a}/i_{p,c}$, is unity for a simple reversible couple. As will be discussed in the following sections, this peak ratio can be strongly affected by chemical reaction coupled to the redox process. The peak potential (E_p) is related to the formal potential of the redox process. The formal potential for a reversible couple is centered between $E_{p,a}$ and $E_{p,c}$:

$$E^0 = \frac{E_{p,a} + E_{p,c}}{2} \quad (2-10)$$

The separation between the peak potential for a reversible couple is given by:

$$\Delta E_p = E_{p,a} - E_{p,c} = 0.059/n \quad \text{V} \quad (2-11)$$

2.4. Working electrode

The performance of the voltammetric method is strongly influenced by the material of the working electrode. The working electrode should provide high signal-to-noise characteristic, in addition to reproducible response. Therefore, its selection depends mainly on two factors: the redox behavior of the electroactive species and the background current over the potential region required for the measurement. Additional considerations include the potential, electrical conductivity, surface reproducibility, mechanical properties, cost, availability, and toxicity. A variety of material has been applied as working electrodes for electroanalysis. The most popular materials are those found in carbon and noble metals, such as platinum and gold.

In this part, screen printed carbon electrodes used as working electrodes in this thesis is illustrated.

2.4.1. Screen printed carbon electrodes

Screen printing technology is a method often used in the fabrication of electrodes for the development of disposable electrochemical biosensors. A screen printed electrode is a planar device based on multiple layers of a graphite-powder-based ink printed on a polyimide, plastic, and epoxy or alumina ceramic substrates. The main advantages of the screen printed electrode consist of simplicity, versatility, modest cost, portability, ease of operation, reliability, small size, and mass production capabilities, which lead to its development in a variety of applications in the electroanalytical field.

2.5. Carbon nanotubes

Carbon Nanotubes (CNTs) are tube-shaped materials, made of carbon, having a diameter measuring on the nanometer scale. The graphite layer appears somewhat like a rolled-up chicken wire with a continuous unbroken hexagonal mesh and carbon molecules at the apexes of the hexagons. CNTs have many structures, differing in length, thickness, and in the type of helicity and number of layers. Although they are formed from essentially the same graphite sheet, their electrical characteristics differ depending on these variations, acting either as metals or as semiconductors. As a group, CNTs typically have diameters ranging from <1 nm up to 50 nm. Their lengths are typically several microns, but recent advancements have made the nanotubes much longer, and measured in centimeters. There are two types of CNTs, namely, single-wall carbon nanotubes (SWCNTs) and multi-wall carbon nanotubes (MWCNTs), which are described below.

2.5.1. Single-wall carbon nanotubes (SWCNTs)

SWCNT is a rolled up tubular shell of graphene sheet as shown in Figure 2.9. In addition, SWCNTs has a diameter of close to 1 nm with a tube length. The body of the tubular shell is mainly made of hexagonal rings of carbon atoms whereas the ends are capped by dome-shaped half-fullerene molecules. The natural curvature in the sidewalls is due to the rolling of the sheet into the tubular structure whereas the curvature in the end caps is due to the presence of topological

(pentagonal ring) defects in the otherwise hexagonal structure of the underlying lattice. The role of the pentagonal ring defect is to give a positive curvature to the surface which helps in closing of the tube at the two ends.

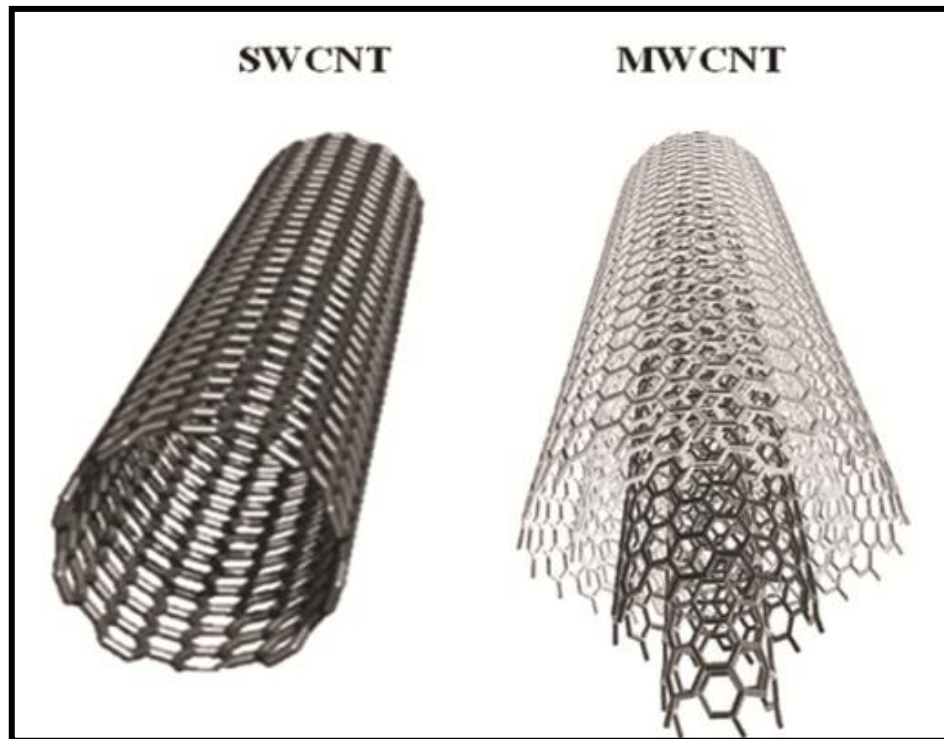


Figure 2.9 Schematic diagrams of single-wall carbon nanotube (SWCNT) and multi-wall carbon nanotube (MWCNT) [34].

2.5.2. Multi-wall carbon nanotubes (MWCNTs)

MWCNT, as presented in Figure 2.9, is a rolled up stack of multi graphene sheets into concentric SWCNTs, with the ends again either capped by half-fullerenes or kept open. The interlayer distance in MWCNTs is close to the distance between graphene layers in graphite, approximately 0.3nm. Moreover, the length and the diameter of these structures differ immensely from SWCNTs.

2.5.3. Properties of carbon nanotubes [35]

The properties of CNTs are determined to a large extent by their dimensional structure. The most important properties of CNTs and their molecular backgrounds are stated below.

- **Chemical reactivity**

The chemical reactivity of CNTs, compared with a graphene sheet, is enhanced as a direct result of the curvature of CNTs surface. The reactivity is directly related to the pi-orbital mismatch caused by an increased curvature. Therefore, a distinction must be made between the sidewall and the end caps of a nanotube. For the same reason, a smaller nanotube diameter results in increased reactivity. Covalent chemical modification of either sidewalls or end caps has showed to be possible. For example, the solubility of CNTs in different solvents can be controlled this way. However, the study of chemical modifications on nanotube behavior is difficult as the nanotube samples are still not pure enough.

- **Electrical conductivity**

Depending on their chiral vector, CNTs with a small diameter are either semiconducting or metallic. The differences in conducting properties are caused by the molecular structure that results in a different band structure and a band gap. The differences in conductivity can be easily derived from the graphene sheet properties. It was showed that a (n, m) nanotube is metallic as accounts that: $n = m$ or $(n - m) = 3i$, where i is an integer, n and m are defining the nanotube. Moreover, the conductivity of CNTs is determined by quantum mechanical aspects and proved to be independence from the nanotube length.

- **Thermal conductivity and resistance**

All nanotubes are the excellent good thermal conductors along the tube, exhibiting a property known as ballistic conduction but good insulators laterally to the tube axis. CNTs are able to transmit up to 6,000 W/m/K at room temperature; comparing this to copper, a metal well known for its good thermal conductivity, which transmits only 385 W/m/K. The temperature stability of CNTs is estimated to be up to 2,800 degrees Celsius in vacuum and about 750 degrees Celsius in air.

- **Mechanical strength**

CNTs are ones of the strong materials known in terms of tensile strength. This strength results from the covalent sp^2 bonds formed between the individual carbon atoms. Besides, CNTs have a very large Young's modulus in their axial direction. The nanotube as a whole is very flexible because of its great length. Therefore, these compounds are potentially suitable for applications in composite

materials that need anisotropic properties. However, CNTs are not nearly as strong under compression. Because of their hollow structure and high aspect ratio, they tend to undergo shattering when placed under compressive, tensional or bending stress.

2.6. Thiol compounds

The thiol compounds are the compounds that contain a carbon-sulphydryl ($-C-SH$ or $R-SH$) group (where R represents an alkane, alkene, or other carbon-containing group of atoms). The $-SH$ functional group itself is referred to as either a thiol group or a sulphydryl group. The thiol compounds such as homocysteine (Hcy), cysteine (Cys), and glutathione (GSH), which are thiol-containing amino acids, play a crucial role in biological metabolism. The structures of Hcy, Cys and GSH are shown in Figure 2.10.

In this part, Hcy used for analyte in this thesis is clearly described.

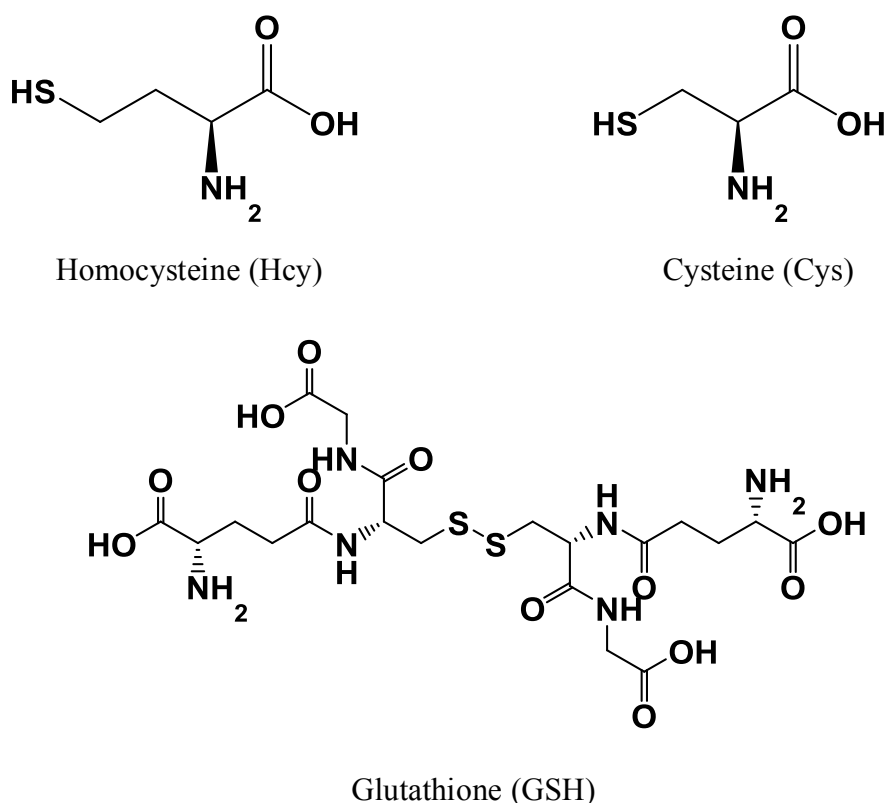


Figure 2.10 Structures of homocysteine (Hcy), cysteine (Cys) and glutathione (GSH).

2.6.1 Homocysteine

Homocysteine (Hcy), sulfur-containing amino acids, shows itself an important role in biochemistry and is a key health indicators or biomarker. In human, Hcy synthesized from methionine (Met) each day is converted to cysteine (Cys) under controlled specific enzyme condition (Figure 2.11). Under normal metabolic circumstances, about 50 % of the Hcy formed is remethylated to methionine. The remethylation of Hcy requires two key enzymes: Met synthase (MS) and methylenetetrahydrofolate reductase (MTHFR). The MS is found in almost all mammalian tissues, uses vitamin B12 as a cofactor and 5-methyltetra-hydrofolate as a methyl donor. The MTHFR is necessary in the formation of 5-methyl-tetrahydrofolate. When there is an excess of protein or Met, a larger proportion of Hcy is metabolised by irreversible transsulfuration pathway, which degrades Hcy to Cys (Figure 2.11). In the transsulfuration, Hcy is first sulfconjugated to cystathionine by cystathionine beta-synthase (CBS), which has been isolated and characterised from human liver. Cystathionine is further cleaved into Cys and alpha-ketobutyrate by cystathionine γ -lyase. Both enzymes need vitamin B6 as a cofactor. Cys may be utilized in the protein synthesis or as a precursor of the antioxidant GSH [36].

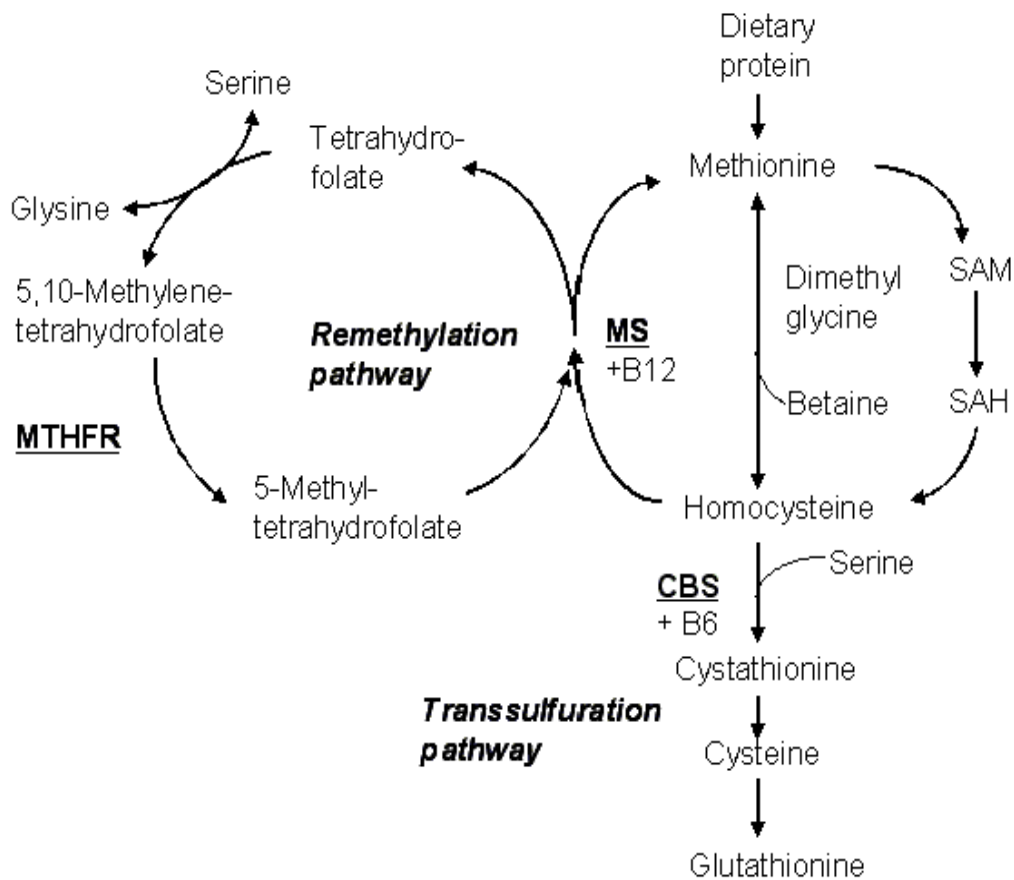


Figure 2.11 Metabolism of homocysteine. (CBS, cystathionine beta-synthase; MS, methionine synthase; MTHFR, methylenetetrahydrofolate reductase; SAH, S-adenosylhomocysteine; SAM, S-adenosylmethionine) [36].

Hcy is a high risk factor for Alzheimer's disease and cardiovascular disease. As such, the analysis of Hcy levels in plasma and urine is of continuing interest to researchers. In humans, normal concentrations of Hcy in plasma and urine range from 6.7 to 14.5 μM and 1.4 to 0.6 μM , respectively [37]. A plasma Hcy concentration greater than 15 μM is termed as hyperhomocysteinemia, which has been classified as moderate (15–30 μM), intermediate (30–100 μM), and severe (> 100 μM) [38]. A high level of Hcy can cause a variety of adverse health effects such as neural tube defects, osteoporosis, and cancer.

2.7. Literature surveys

2.7.1 Conventional methods for Hcy detection

The analytical method for Hcy has gained increasing interest. Current methods for the determination of Hcy levels are provided with several separation methods including gas chromatography (GC), high performance liquid chromatography (HPLC), and capillary electrophoresis (CE). These separation methods are commonly coupled with mass spectrometry (MS), electrochemical (EC), ultraviolet-visible (UV-vis), fluorescent detection or even a simple mean like the naked eye detection.

In 2003, Frick *et al.* developed the HPLC method for rapid and sensitive measurement of total Hcy [39]. Hcy was clearly distinguishable from Cys and cysteinylglycine (CysGly) with the retention time of 2.2 min and total analysis time of 6 min. Linearity was obtained in the concentration range of 0.6-100 μM and limit of detection was 0.5 μM . Tests of recovery and precision were satisfactory, as well as the results were compared with a commercial available assay method.

In 2004, Lawrence *et al.* demonstrated the use of a carbon-nanotube paste (CNTP) electrode as an effective means for the determination of Hcy [40]. The analytical parameters were evaluated with a linear range from 5 to 200 μM and a detection limit of 4.6 μM . In comparison to the carbon paste electrode, the increased reactivity of the CNTP electrodes for the determination of Hcy provided means of significantly lowering the overpotential for the oxidation of the thiol moiety and enhanced the signal-to-noise characteristics.

In 2005, Chwatko and Jakubowski described a sensitive assay for the determination of Hcy-thiolactone [41]. Firstly, plasma Hcy-thiolactone was separated from macromolecules by ultrafiltration. It was then selectively extracted with chloroform/methanol. Next, purification of Hcy-thiolactone was accomplished by HPLC using a cation exchange column. After postcolumn derivatization with *o*-phthaldialdehyde, the detection and quantification were monitored by fluorescence. The calibration curve was obtained for the analysis of Hcy-thiolactone over the concentration range from 1 to 40 nM. The limit of detection was 0.36 nM.

In 2006, Zhang *et al.* reported a simple colorimetric method for the determination of Hcy and Cys using azo dyes containing an aldehyde group [42].

Under neutral pH condition, the derivatives thiazolidines or thiazinanes were obtained from the reaction of the azo dyes containing an aldehyde group with Hcy or Cys. The recognition of Hcy and Cys offered apparent color changes from pink to yellow, which was easily observed by the naked eye. This approach was selective and sensitive for Hcy and Cys detection without the interference of other amino acids.

In 2007, Agüí *et al.* developed construction of a colloidal gold-cysteamine-carbon paste electrode ($\text{Au}_{\text{coll}}\text{-Cyst-CPE}$), for the electrochemical determination of Hcy [43]. In this work, a colloidal gold-cysteamine-carbon paste electrode, $\text{Au}_{\text{coll}}\text{-Cyst-CPEs}$, was constructed for the improved electrochemical determination of Hcy. The capability of this modified electrode to be used as an amperometric detector in the HPLC determination of thiol derivatives is demonstrated. Calibration graphs were constructed for all the separated compounds. Detection limits ranged between 20 nM for Cys and 120 nM for penicillamine, with a value for Hcy of 30 nM. These values compare advantageously with those achieved with previously reported HPLC methods using electrochemical, UV, fluorescence and MS detection modes. The developed method was applied to the determination of Cys and Hcy in serum samples with good results.

In 2009, Hui Lin *et al.* presented the development of a simple, sensitive, and selective-detection system for Hcy based on the combination of fluorosurfactant-capped gold nanoparticles (FSN-AuNPs) and o-phthalaldehyde (OPA) [44]. The proposed assay utilizes FSN-AuNPs as extractors for Hcy and Cys, which can then be collected by centrifugation. As long as the Hcy and Cys are isolated from the initial sample, they can be liberated from the NP surface by 2-mercaptoethanol (2-ME). The derivatization of released Hcy with OPA/2-ME has a strong fluorescence maximum at 485 nm, whereas the derivatization of released Cys with the same reagent shows an extremely weak fluorescence maximum at 457 nm. As a result, the selectivity of this system is more than 100-fold for Hcy over any amino thiols when excited at 370 nm. The extraction and derivation efficiencies are monitored as functions of the concentration of FSN-AuNPs and OPA, respectively. The proposed system has a detection limit of 180 nM at a signal-to-noise ratio of 3 for Hcy. This study validates the applicability of this system by analyzing the amount of Hcy in urine samples.

In 2011, Leesutthiphonchai *et al.* reported rapid, simple, and selective determination of Hcy levels in human plasma using silver nanoparticles (AgNPs) [45]. Under optimum conditions, the red-shifted band resulting from Hcy-induced aggregation of AgNPs was observed at 525 nm, whereas Cys gave no significant wavelength shift. The difference in the cross-linking rate between Hcy and Cys was used as the basis for developing a selective probe for Hcy and allowed the detection of Hcy in the linear range of 2–12 μM ($R^2 = 0.9936$). The limits of detection and quantification were found to be 0.5 μM and 1.7 μM , respectively. Furthermore, the current AgNP-based method was successfully applied for the actual determination of Hcy levels in biological human plasma samples, where the experimentally determined levels were within the error range of the levels measured for the same samples using the traditional clinical diagnostic chemiluminescence microparticle immunoassay (CMIA).

2.7.2 Electrochemiluminescence (ECL) with carbon nanotube modified electrode

Carbon nanotubes (CNTs) have been exploited as electrode materials due to their outstanding electronic, chemical, and mechanical properties. CNTs-modified electrodes can exhibit excellent abilities compared with bare electrodes and have been widely used in ECL systems.

In 2006, Choi *et al.* developed a highly sensitive and stable tris (2,2'-bipyridyl) ruthenium(II) ($\text{Ru}(\text{bpy})_3^{2+}$) ECL based on CNTs dispersed in mesoporous composite films of sol-gel titania and perfluorosulfonated ionomer (Nafion) [46]. The hydrophobic CNTs in the titania–Nafion composite films coated on a glassy carbon electrode certainly increased the amount of $\text{Ru}(\text{bpy})_3^{2+}$ immobilized in the ECL sensor by adsorption of $\text{Ru}(\text{bpy})_3^{2+}$ onto CNTs surface. The electrocatalytic activity towards the oxidation of hydrophobic analytes, and the electronic conductivity of the composite films were also enhanced. Therefore, the present ECL sensor based on the CNTs–titania–Nafion showed improved ECL sensitivity for tripropylamine (TPA) compared to the ECL sensors based on both titania–Nafion composite films without CNTs and pure Nafion films. The present $\text{Ru}(\text{bpy})_3^{2+}$ ECL sensor based on the

MWCNT–titania–Nafion composite gave a linear response ($R^2 = 0.999$) for TPA concentration from 50 nM to 1.0 mM with a remarkable detection limit ($S/N = 3$) of 10 nM, while the ECL sensors based on titania–Nafion composite without MWCNTs, pure Nafion films, and MWCNTs–Nafion composite gave a detection limit of 0.1 μ M, 1 μ M, and 50 nM, respectively. The present ECL sensor showed outstanding long-term stability (no signal loss for 4 months).

In 2007, Huang *et al.* reported a novel method for immobilization of CNTs on the surface of graphite electrode [47]. This work further found that superoxide ion was electrogenerated on this CNTs-modified electrode, which can react with sulfide ion combining with a weak but fast ECL emission, and this weak ECL signal could be enhanced by the oxidative products of rhodamine B. In addition, the rate constant of this electrochemical reaction k_0 was investigated and confirmed that the speed of electrogenerating superoxide ion was in accordance with the subsequent fast CL reaction. Under the optimum conditions, the enhancing ECL signals were linear with the sulfide ion concentration in the range from 6.0×10^{-10} to 1.0×10^{-8} M, and a 2.0×10^{-10} M detection limits (3σ) was achieved. In addition, the proposed method was successfully used to detect sulfide ion in environmental water samples

In 2008, Lin *et al.* showed the advantages of electrocatalytic activity of carbon nanotube modified glassy carbon electrode and the advantages of Nafion film to construct glucose biosensors based on luminol ECL reaction [48]. The performance of the ECL system with respect to pH value of the solution, luminol concentration, selectivity and stability of the biosensor were investigated. The biosensor had also been applied in real sample determinations. Under the optimum condition, the linear response range of glucose was found to be 5.0×10^{-6} to 8.0×10^{-4} M, and the detection limit was 2.0×10^{-6} M. The present carbon-nanotube/Nafion biocomposite glucose oxidase ECL biosensor showed excellent properties for sensitive determination for glucose with good reproducibility and stability, and it has been used to determine the glucose concentrations in real serum samples with the satisfactory results.

In 2009, Hua *et al.* reported a novel analytical method based on ECL of CdTe QDs using CNTs modified glass carbon (GC) electrode [49]. It was found that the CNTs film on the GC electrode could greatly enhance the ECL intensity of

CdTe QDs dispersed in aqueous solution, and the ECL peak potential and ECL onset potential both shifted positively. Influences of some factors on the ECL intensity were investigated using CNTs modified GC electrode, and a high sensitive method for the determination of methimazole was developed under the optimal conditions. The ECL intensity decreased linearly in the concentration range of 1.0×10^{-9} to 4.0×10^{-7} M for methimazole with the relative coefficient of 0.995, which showed finer sensitivity than that at a bare electrode. Thus, CNTs modified electrode would have a great merit to expand the application of QD ECL.

In this research, we propose a novel strategy for Hcy determination based on the quenching effect of TGA-capped CdTe QDs ECL using the CNTs-modified screen-printed electrodes (SPCNTs), which are simple, rapid, sensitive, inexpensive, flexible to design, and easy to fabricate and modify.

CHAPTER III

EXPERIMENTAL

The information about the instruments and equipments, the chemicals, the chemical preparation, the synthetic quantum dots preparation, the electrode modification and the detection method in this work is thoroughly described in this chapter.

3.1 Instruments and equipments

3.1.1 Preparation of CdTe quantum dots

The instruments and equipments for the preparation of CdTe quantum dots are listed in Table 3.1.

Table 3.1 List of instruments and equipments for the preparation of CdTe quantum dots.

Instruments / equipments	Suppliers
Temperature controller	Shinko Technos, Japan
Heating mantle	Glas-col, USA
Vacuum pump	Labconco, UK
Hot plate stirrer, HL HS-115	Harikul Science, Thailand
Magnetic stirring bars	SGS ICS, Switzerland
Milli-Q ultrapure water purification system, R \geq 18.2 M Ω ·cm	Millipore, USA
A tabletop centrifuge	Andreas Hettich GmbH, Germany
Analytical balance, Mettler AT 200	Mettler, Switzerland
Universal indicator test papers, pH 1-14	Merck, Germany
Syringe	
Schlenk line	
Three-necked round bottom flask	

3.1.2 Characterization of CdTe quantum dots

The instruments and equipments for the characterization of CdTe quantum dots are listed in Table 3.2.

Table 3.2 List of instruments and equipments for the characterization of CdTe quantum dots.

Instruments / equipments	Suppliers
UV-Vis spectrometer, 8453E UV-Vis	Agilent, USA
Luminescence spectrometer, LS 45	Perkin Elmer, USA
Transmission electron microscope, JEM-2100	JEOL, Japan
Infrared Spectrometer, Impact 410	Nicolet, USA
Ultrasonic bath, ULTRASONIK 28H	ESP Chemicals, USA
Milli-Q ultrapure water purification system, R \geq 18.2 M Ω ·cm	Millipore, USA
Lacey carbon film/copper grids, Type 300 mesh	Electron Microscopy Sciences, USA
Quartz cuvette	

3.1.3 Fabrication of carbon nanotubes-modified screen-printed carbon electrodes (SPCNTes)

The instruments and equipments used in the fabrication of SPCNTes are listed in Table 3.3.

Table 3.3 List of instruments and equipments involved in the fabrication of SPCNTes.

Instruments / equipments	Suppliers
Screen-printed blocks	Chaiyaboon, Thailand
Hot air oven	Memmert, USA
Universal indicator test papers, pH 1-14	Merck, Germany

Ultrasonic bath, ULTRASONIK 28H	ESP Chemicals, USA
---------------------------------	--------------------

3.1.4 Electrochemiluminescence of CdTe quantum dots sensor based on the SPCNTEs for determination of homocysteine (Hcy)

The instruments and equipments for determination of Hcy using electrochemiluminescence of CdTe quantum dots (CdTe QDs ECL) sensor based on the SPCNTEs are shown in Table 3.4.

Table 3.4 List of instruments and equipments connected to the CdTe QDs ECL sensor for Hcy determination.

Instruments / equipments	Suppliers
Potentiostat	Autolab, The Netherlands
Photomultiplier tube, model 98285B	Electron Tubes, UK
Power supply, Thorn-EMI model PM20D	Electron Tubes, UK
Digital multimeter, UNI-T UT60F	UNI-Trend Technology, Hong Kong
Black box (custom-built light tight)	Homemade
Ag/AgCl reference electrode	Bioanalytical Systems, USA
Platinum wire counter electrode	Goodfellow, UK
Vortex mixer, Mixer Uzusio VTX-3000L	LMS, Japan
A tabletop centrifuge	Andreas Hettich GmbH, Germany
Analytical balance, Mettler AT 200	Mettler, Switzerland
Vacuum pump	GAST Manufacturing, USA
Nylon membrane filters 0.2 μm 47 mm	Whatman, UK
pH meter, 827 pH Lab	Metrohm, Switzerland
Autopipette and tips	Eppendorf, Germany
Cuvette quartz cell	
Glasswares	

3.2 Chemicals

3.2.1 Preparation of CdTe quantum dots

The chemicals for the preparation of CdTe quantum dots are listed in Table 3.5.

Table 3.5 List of chemicals for the preparation of CdTe quantum dots.

Chemicals	Suppliers
Cadmium chloride	Sigma-Aldrich, Germany
Sodium tellurite	Sigma-Aldrich, Germany
Sodium borohydride	Sigma-Aldrich, Germany
Tri-sodium citrate	Sigma-Aldrich, Germany
Thioglycolic acid	Sigma-Aldrich, Germany
Sodium hydroxide	Merck, Germany
Acetone	Merck, Germany
Nitrogen gas	Linde Public, Thailand
Liquid nitrogen	Linde Public, Thailand

3.2.2 Fabrication of carbon nanotubes-modified screen-printed carbon electrodes (SPCNTEs)

The chemicals for the fabrication of SPCNTEs are listed in Table 3.6.

Table 3.6 List of chemicals for the fabrication of SPCNTEs.

Chemicals	Suppliers
Multi-walled CNTs	Nanomaterials Research Unit at Chiangmai University, Thailand

Sulfuric acid 95-97%, 1.84 g mL ⁻¹	Merck, Germany
Nitric acid 65%, 1.39 g mL ⁻¹	Merck, Germany
Silver ink, Electrodag 7019	Acheson, USA
Carbon ink, Electrodag PF-407C	Acheson, USA

3.2.3 Electrochemiluminescence of CdTe quantum dots sensor based on the SPCNTEs for determination of homocysteine (Hcy)

The chemicals for determination of Hcy using CdTe QDs ECL sensor based on the SPCNTEs are listed in Table 3.7.

Table 3.7 List of chemicals for determination of Hcy using CdTe QDs ECL sensor based on the SPCNTEs

Chemicals	Suppliers
L-Homocysteine	Sigma-Aldrich, Germany
L-Cysteine	Sigma-Aldrich, Germany
L-Glutathione	Sigma-Aldrich, Germany
Potassium dihydrogen phosphate	Sigma-Aldrich, Germany
di-Sodium hydrogen phosphate	Sigma-Aldrich, Germany
Potassium peroxodisulfate	Merck, Germany
Ethylenediaminetetraacetic acid disodium salt dehydrate (EDTA) 98-101%	Sigma-Aldrich, Germany
Tris(2-carboxyethyl)phosphine hydrochloride	Sigma-Aldrich, Germany
Perchloric acid 70-72%	Merck, Germany
Sodium chloride	Merck, Germany
Potassium chloride	Univar, Australia
Ammonium chloride	Sigma-Aldrich, Germany
Ammonium hydroxide	Sigma-Aldrich, Germany

Magnesium sulfate	Sigma-Aldrich, Germany
Sodium sulfate	Sigma-Aldrich, Germany

3.3 Chemical preparations

3.3.1 Preparation of CdTe quantum dots

- **0.01 M cadmium chloride solution**

A 0.01 M cadmium chloride solution was prepared by dissolving 0.0183 g of cadmium chloride in 10 mL of Milli-Q water.

- **1 M sodium hydroxide solution**

A 1 M sodium hydroxide solution was prepared by dissolving 2 g of sodium hydroxide in 50 mL of Milli-Q water.

- **0.01 M sodium tellurite solution**

A 0.01 M sodium tellurite solution was prepared by dissolving 0.0222 g of sodium tellurite in 10 mL of Milli-Q water.

3.3.2 Preparation of stock standard solution for determination of Hcy using CdTe QDs ECL sensor

- **0.1 M phosphate buffer solution (PBS)**

A 0.1 M phosphate buffer solution (PBS) was prepared by mixing 0.1 M potassium dihydrogen phosphate solution and 0.1 M di-sodium hydrogen phosphate solution as shown in table 3.8 and then adjusted pH at 8 by adding sodium hydroxide and hydrochloric acid.

Table 3.8 Preparation of 0.1 M phosphate buffer solution (PBS).

Desired pH	Volume of 0.1 M potassium dihydrogen phosphate solution (mL)	Volume of 0.1 M di-sodium hydrogen phosphate solution (mL)
5.0	99.2	0.8
6.0	88.9	11.1
7.0	41.3	58.7
8.0	3.7	96.3

- **10 mM stock solution of homocysteine solution**

A 10 mM stock solution of homocysteine was prepared by dissolving 0.0136 g of homocysteine in 10 mL of 0.1 M PBS.

- **10 mM stock solution of cysteine solution**

A 10 mM stock solution of cysteine was prepared by dissolving 0.0122 g cysteine in 10 mL of 0.1 M PBS.

- **10 mM stock solution of glutathione solution**

A 10 mM stock solution of glutathione was prepared by dissolving 0.0306 g of glutathione in 10 mL of 0.1 M PBS.

- **250 mM stock solution of potassium peroxodisulfate solution**

A 250 mM stock solution of potassium peroxodisulfate was prepared by dissolving 3.3791 g of potassium peroxodisulfate in 50 mL of Milli-Q water.

3.4 Preparation of CdTe quantum dots

The thiol-capped CdTe QDs were synthesized using TGA as stabilizing agent according to the hydrothermal method. The synthesis procedure can be divided into eight steps:

- (i) Firstly, 38 mL of Milli-Q water and 10 mL of 0.01 M CdCl₂ were transferred to a three-necked round bottom flask under nitrogen gas flow.
- (ii) 10 μL of TGA stabilizer was added quickly under N₂ atmosphere.
- (iii) The pH of this solution was adjusted to 11.0 by dropwise addition of 1 M NaOH.
- (iv) After the color of solution became clear, 55.5 mg tri-sodium citrate and 2 mL of 0.01 M Na₂TeO₃ were respectively added into this solution.
- (v) 3.0 mg NaBH₄ was also added, and the solution was de-aerated by highly pure N₂ bubbling for 10 min.

- (vi) About 25 mL of this mixture was transferred to a reaction kettle, the mixture solution was heated at 180 °C and refluxed for 60 min. As a result, thiol-capped CdTe QDs could be obtained.
- (vii) Afterward, the resulted products were precipitated by acetone. The superfluous Cd²⁺, and TGA were removed by centrifugation at 3000 rpm for 10 min.
- (viii) Finally, the resultant precipitate was re-dispersed in water and then re-precipitated for more than two times by a copious amount of acetone. The products were kept in the dark for further use.

3.5 Characterization of CdTe quantum dots

The ultraviolet-visible (UV-Vis) spectra were acquired on the UV-Vis spectrometer (8453E UV-Vis, Agilent, USA) using a 1.0 cm quartz cell. The photoluminescence (PL) spectra were measured with luminescence spectrometer (LS 45, Perkin Elmer, USA) and the excitation wavelength was fixed at 390 nm. Infrared (IR) spectra were recorded on IR spectrometer (Impact 410, Nicolet, USA) in the range of 400-4000 cm⁻¹ for structural characterization of the prepared CdTe quantum dots. Transmission electron microscopy (TEM) images were obtained on transmission electron microscope (JEM-2100, JEOL, Japan) for analysis of size, morphology and particle size distributions of CdTe quantum dots. For the TEM measurements, one drop of a dilute CdTe quantum dots in water was placed onto a Lacey carbon film coated copper grid and dried at room temperature.

3.6 Fabrication of carbon nanotubes-modified screen-printed carbon electrodes (SPCNTes)

Before modifying the electrode, CNTs were functionalized by dispersing 1.0 g of CNTs in 50 mL of a 3:2 (v/v) of concentrated H₂SO₄ and HNO₃. The mixture was then agitated by ultrasonic wave for 12 h. After that, the CNT suspension was washed with Milli-Q water until the pH of the mixture approached 7, filtered and dried at 80 °C [18].

SPCNTEs used for working electrode in ECL detection (Figure 3.1) were prepared in-house using screen-printing procedure, as shown in Figure 3.2.

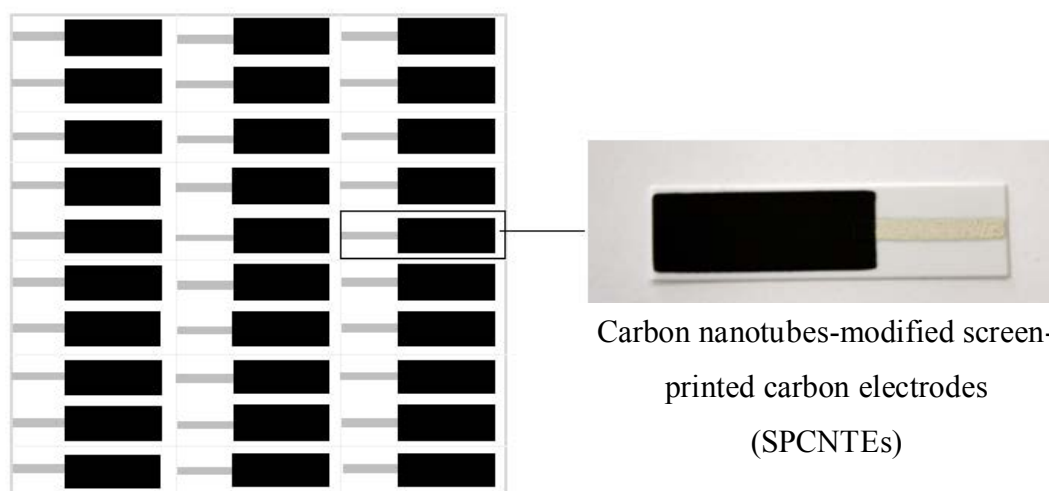


Figure 3.1 Carbon nanotubes-modified screen-printed carbon electrodes (SPCNTEs).

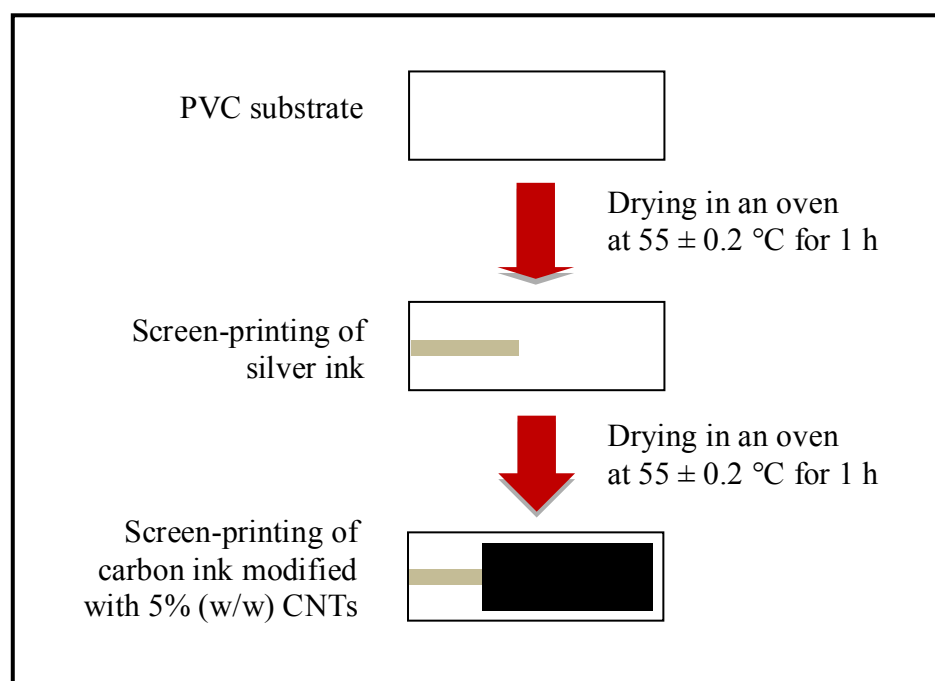


Figure 3.2 Schematic illustration of the screen-printing procedure of the SPCNTEs.

Silver ink (Electrodag 7019, Acheson, USA) was printed onto the polyvinyl chloride (PVC) substrate and dried in an oven at 55 ± 0.2 °C for 1 h. The 5 % (w/w) CNTs was mixed with carbon ink (Electrodag PF-407C, Acheson, USA) to form the homogenized ink, which was then screen-printed onto the silver conducting part and dried in an oven at 55 ± 0.2 °C for 1 h.

3.7 Electrochemiluminescence of CdTe quantum dots (CdTe QDs ECL) sensor based on the SPCNTEs for determination of homocysteine (Hcy)

CdTe QDs ECL emissions were excited with cyclic voltammetry using potentiostat (Autolab, The Netherland). The electrochemical cell with three-electrode system consisted of SPCNTEs as the working electrode, a platinum wire as the counter electrode, and an Ag/AgCl (saturated KCl) electrode as the reference electrode. For detecting ECL, the cell was placed directly in front of a photomultiplier tube (PMT, model 98285B, Electron Tubes, UK) biased at -800 V. The sample cell, PMT, and voltage divider were encased in a custom-built light tight while the detector output was recorded on a PC (Pentium IV) via a USB/RS-232 interfaced to the detector. The operational potential for the PMT was provided by a stable power supply (Thorn-EMI model PM20D, Electron Tubes, UK). The multimeter (UNI-T UT60F, Hong Kong) was used to determine the peak. The electrochemiluminescence system was shown in Figure 3.3.

CdTe QDs ECL assay was achieved in PBS containing $K_2S_2O_8$ as a co-reactant and CdTe QDs. CdTe QDs ECL intensity was recorded at the PMT. According to the results, PMT gave the proportional output with ECL intensity while the analytical signal of the ECL was at the maximal output potential corresponding to peak maximum. Certain volume of various concentrations of homocysteine standard solutions or sample solutions were added into the ELC cell and the quenched ECL intensities were recorded corresponding to the concentration of homocysteine.

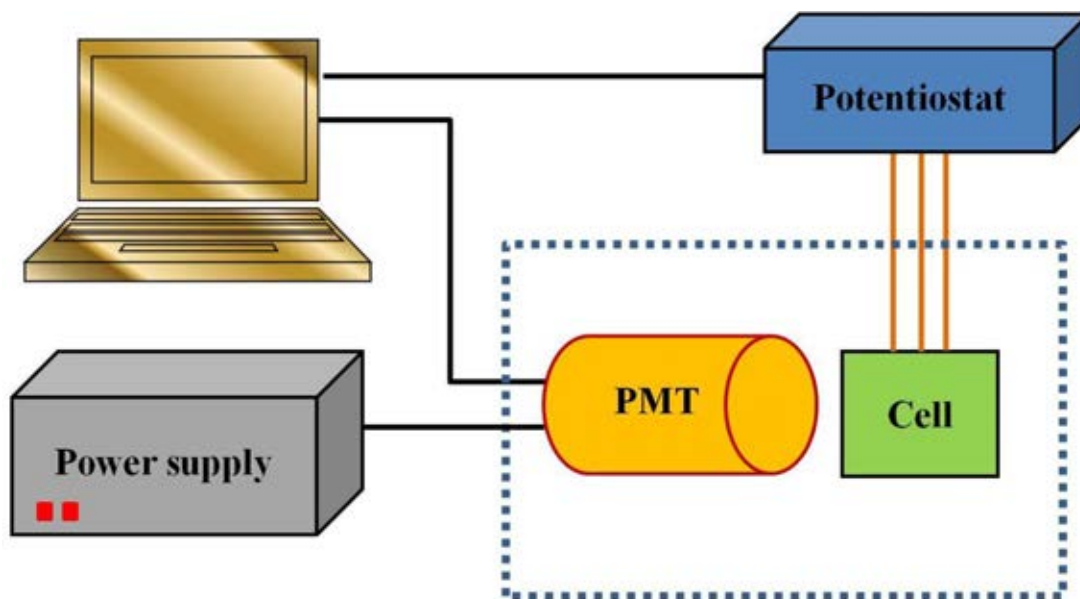


Figure 3.3 Schematic diagram of the Electrogenerated Chemiluminescence system.

3.8 Optimization of CdTe QDs ECL conditions

3.8.1 The effect of potential

The influence of potential on the CdTe QDs ECL at SPCNTEs was investigated by variation of potential at -1.0, -1.1, -1.2, -1.3, -1.4, -1.5 and -1.6 V.

3.8.2 The effect of scan rate

The effect of scan rate on the CdTe QDs ECL at SPCNTEs was studied by variation of scan rate at 50, 100, 150, 200, 250, 300, 350, 400, 450 and 500 mVs⁻¹.

3.8.3 The effect of step potential

The effect of step potential on the CdTe QDs ECL at SPCNTEs was examined by variation of step potential at 15, 20, 25, 30, 35 and 40 mV.

3.8.4 The effect of concentration of CdTe QDs

The effect of the concentration of CdTe QDs solution on the ECL intensity was explored at 1, 3, 4, 5, 6, 7, 8, 10 and 11 μ M.

3.8.5 The effect of concentration of $K_2S_2O_8$ co-reactant

The effect of the concentration of $K_2S_2O_8$ co-reactant on the CdTe QDs ECL intensity was considered at 0.5, 1, 5, 10, 15, 20, 25 and 30 mM.

3.8.6 The effect of PBS pH

The effect of PBS on the intensity of CdTe QDs ECL was studied in the range of pH 5–10 by adjusting the PBS pH with sodium hydroxide and hydrochloric acid.

3.9 Reproducibility and stability study

For reproducibility and stability study, the CdTe QDs ECL at different SPCNTEs were investigated using homocysteine standard solutions at concentration of 5, 15 and 30 μM (10 cycle measurements for each concentration) under the optimal condition.

3.10 The analytical performance

3.10.1 Linearity

The standard solution of homocysteine in the concentration range of 5 to 35 μM was analyzed by quenching effect of homocysteine on the CdTe QDs ECL at SPCNTE under the optimized conditions. The average intensity for triplicate measurements ($n=3$) were used to plot calibration curve which linear range can be obtained.

3.10.2 Limit of detection (LOD) and Limit of quantification (LOQ)

LOD was determined statistical method from the calibration curve in the range of 5 to 35 μM and calculated from $3S_{\text{blank}}/S$, where S_{blank} is the standard deviation of blank measurement ($n = 3$) and S is the slope of the linearity or the sensitivity of the method. Moreover, LOD were also obtained by experimental method consisted of analyzing a series of sample solutions containing increasingly

lower concentration of analyte and LOD is the lowest concentration at which the signal can be measured.

LOQ was determined statistical method from the calibration curve in the range of 5 to 35 μM and calculated from $10S_{\text{blank}}/S$, where S_{blank} was the standard deviation of blank measurement ($n = 10$) and S was the slope of the linearity or the sensitivity of the method.

3.11 Interference effect

To study the selectivity of Hcy determination using CdTe QDs ECL at SPCNTEs, the effect of other compounds commonly found in biological samples that could act as potential sources of interference on the quenching effect of CdTe QDs ECL, cysteine and glutathione, were tested. 20 μM Hcy solutions in presence of cysteine and glutathione was experimentally studied which cysteine and glutathione concentration was varied in the range of 20 to 500 μM .

3.12 Real sample analysis

3.12.1 Determination of homocysteine in human urine sample

Fresh human urine sample was collected from healthy volunteer, and the diagnosis was conducted immediately after the sample collection. The portion of 2 mL of human urine sample was transferred to a centrifuge tube, 1 mL of 0.1 M EDTA and 0.1 mL of 0.2 M TCEP were added. Afterward, the mixture was kept at 60 $^{\circ}\text{C}$ for 30 min, which was then allowed to cool to room temperature. The sample was gently vortex-mixed with 0.4 mL of 3.0 M perchloric acid solution, incubated for 10 min at room temperature and centrifuged at 6,000 rpm for 10 min. The clear supernatant was filtered through 0.22 μm filter and diluted when required to use for further analysis. Then the standard addition method was used to determine homocysteine in human urine sample.

3.12.2 Determination of homocysteine in artificial urine sample

The artificial urine sample was prepared by dissolving 0.616 g of sodium chloride, 0.475 g of potassium chloride, 0.194 g of ammonium chloride, 0.002 g of ammonium hydroxide, 0.046 g of magnesium sulfate and 0.241 g of sodium sulfate in 100 mL Milli-Q water. Then the standard addition method was performed to determine homocysteine in artificial urine sample.

3.12.3 Accuracy and precision study

For accuracy study, the urine sample was spiked with homocysteine standard solution at the concentration of 5, 15 and 30 μM . The spiked sample was prepared in triplicate and analyzed in triplicate runs. The accuracy is assessed in terms of recovery, using the following formula:

$$\% \text{ Recovery} = \frac{\text{Spiked}_{\text{matrix}}}{\text{Spiked}_{\text{blank}}} \times 100$$

For precision study, the repeatability of the developed method was examined by ten replicate measurements of solutions containing 5, 15 and 30 μM homocysteine standard solution. The signal intensities were measured. The precision is assessed in terms of the relative standard deviation (RSD), using the following formula:

$$\% \text{ RSD} = \frac{\text{Standard deviation}}{\text{Mean}} \times 100$$

CHAPTER IV

RESULTS AND DISCUSSION

4.1 Preparation of TGA-capped CdTe quantum dots

The mechanism for the synthesis of TGA-capped CdTe quantum dots was proposed [17] as shown in Figure 4.1.

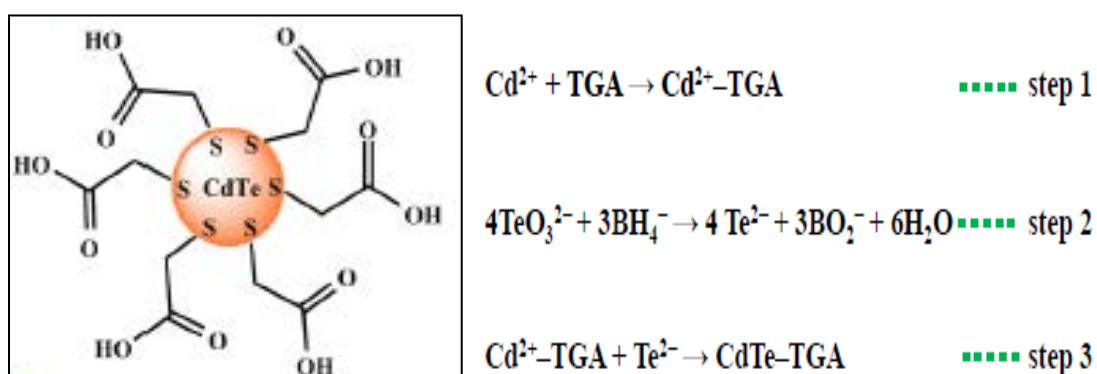


Figure 4.1 Schematic diagram showing the mechanism for the preparation of TGA-capped CdTe quantum dots

As illustrated in Figure 4.1, the synthetic CdTe quantum dots were prepared using cadmium chloride and sodium tellurite as precursors and using thioglycolic acid (TGA) as capping ligand according to the hydrothermal [17]. The TGA capping ligands attached to the surface of CdTe quantum dots are found to be important to the formation of the nanocrystals because it can prevent the aggregation of CdTe quantum dot nanocrystals.

The mechanism above can be used to describe the formation of TGA-capped CdTe QDs as follows. Firstly, cadmium-TGA complexes ($\text{Cd}^{2+}\text{-TGA}$) were formed in the solution as demonstrated in Step 1. When the sodium tellurite (TeO_3^{2-}) was added into the solution, it was reduced by sodium borohydride (NaBH_4) to provide telluride ion (Te^{2-}) in Step 2. Then telluride ions reacted with the $\text{Cd}^{2+}\text{-TGA}$ complexes, resulting in the formation of TGA-capped CdTe as indicated in Step 3.

4.2 Characterization of CdTe quantum dots

4.2.1 UV–Vis and PL spectroscopy

TGA-capped CdTe QDs were characterized using UV–Vis and PL spectroscopy to confirm their particle sizes and concentrations. As shown in Figure 4.2, the first UV–Vis absorption peak and maximum PL emission peak of TGA-capped CdTe QDs appeared were at 505 nm and 587 nm, respectively. The estimated particle size of TGA-capped CdTe QDs was 2.47 nm as calculated in virtue of the following empirical equation [50].

$$D = (9.8127 \times 10^{-7}) \lambda^3 - (1.7147 \times 10^{-3}) \lambda^2 + 1.0064 \lambda - 194.84$$

where D is the average diameter (nm) of a given TGA-capped CdTe QDs

λ is the wavelength (nm) of the first excitonic absorption peak from the UV–Vis spectra.

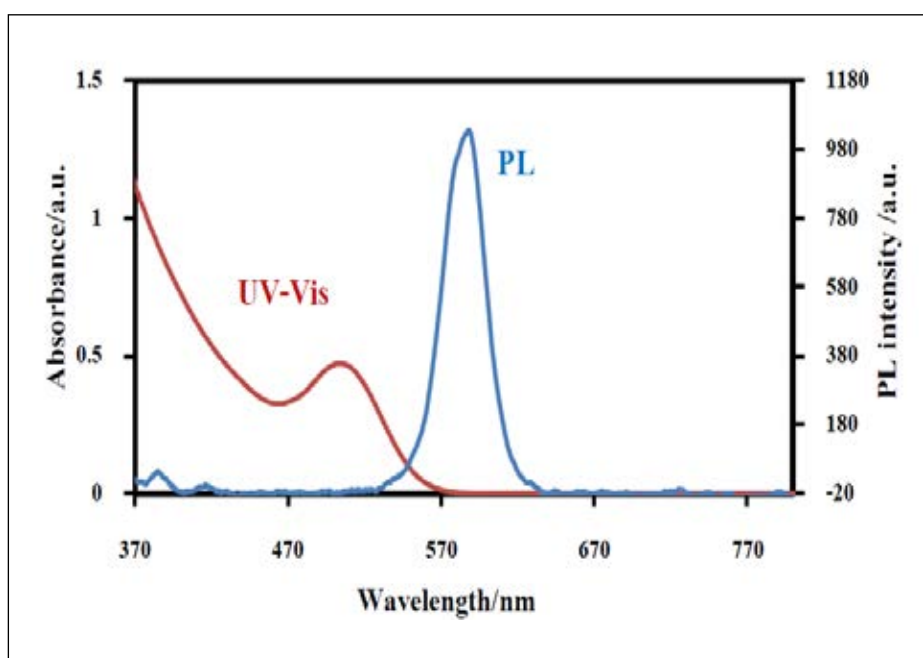


Figure 4.2 PL emission (blue) and UV–Vis absorption spectra (red) of TGA-capped CdTe QDs.

Moreover, the concentration of TGA-capped CdTe QDs solution was calculated upon the data from UV–Vis absorption spectra because it is difficult to determine the concentration of prepared TGA-capped CdTe QDs by gravimetric method. This is because, in QDs, the number of ligands on the surfaces is difficult to identify and may vary under different conditions. Measurements based on gravimetric methods using ligands coated nanocrystals are accurate only when the interactions between nanocrystals and ligands are strong enough to withstand necessary purification procedures. Therefore, the concentration of TGA-capped CdTe QDs was calculated according to the Lambert-Beer's law equation as follow:

$$A = \epsilon Cl$$

where A is the absorbance at the peak position of the of the first excitonic absorption peak of the UV–Vis spectra for CdTe.

C is the molar concentration of TGA-CdTe QDs.

l is the path length (1 cm) of the radiation

ϵ is the molar extinction coefficient at the first excitonic absorption peak, which could be obtained from the formula $\epsilon = 10043 \times D^{2.12}$.

Therefore, the concentration of as-synthesized TGA-CdTe QDs was calculated as 7.39×10^{-3} M.

4.2.2 Transmission electron microscopy

Morphologies and particle sizes of TGA-capped CdTe QDs were observed clearly by TEM image (Figure 4.3). These results showed that the average size of TGA-capped CdTe QDs was approximately 2.53 nm, which is considered close to the value of 2.47 nm calculated from the empirical formula mention aboved. The validity of the calculation allowed us to use the calculated size which is more convenient to obtain.

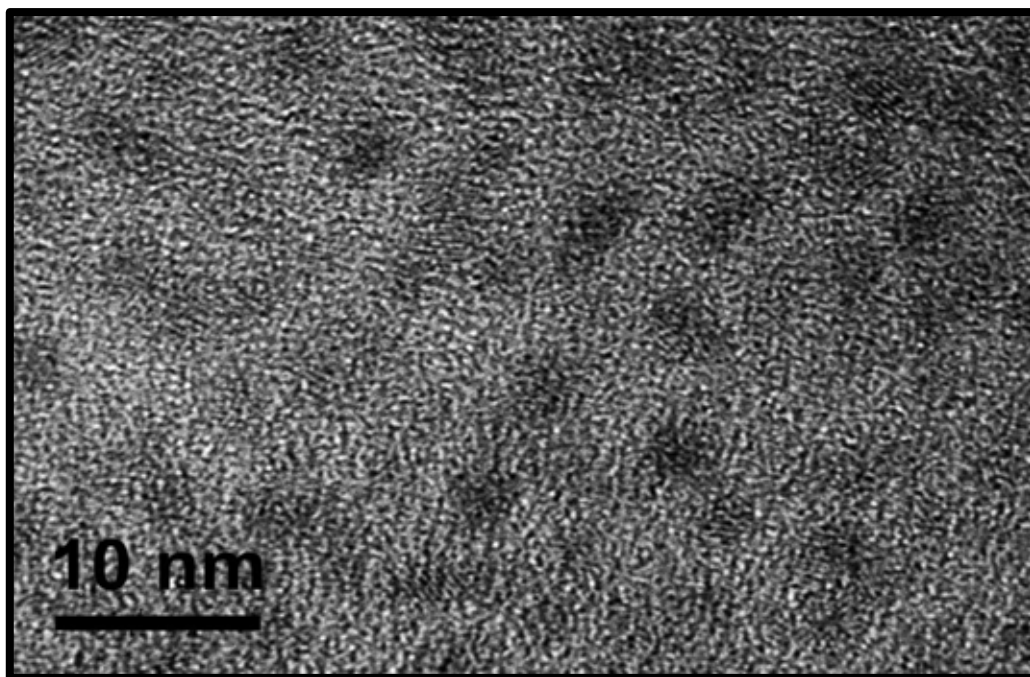


Figure 4.3 TEM image of TGA-capped CdTe QDs.

4.2.3 Infrared spectroscopy

The IR spectra were used to characterize the structure and composition of TGA-capped CdTe QDs. As shown in Figure 4.4A, TGA displayed a peak at 2598 cm^{-1} for stretching vibration of S-H bond, which lessened in the spectrum of TGA-capped CdTe QDs (Figure 4.4A). Consequently, it could be predicted that the Cd-S bonds were formed between TGA and CdTe core. Furthermore, the asymmetric vibration of carboxyl group of TGA shifted from 1717 to 1575 cm^{-1} and the symmetric vibration of the carboxyl anion at 1378 cm^{-1} appeared in the spectrum of TGA-capped CdTe QDs were indications that the carboxyl group of TGA turned into its corresponding anion. Consequently, the structure of TGA-capped CdTe QDs exhibited the characters of cadmium-rich CdTe core covered with excess TGA²⁻.

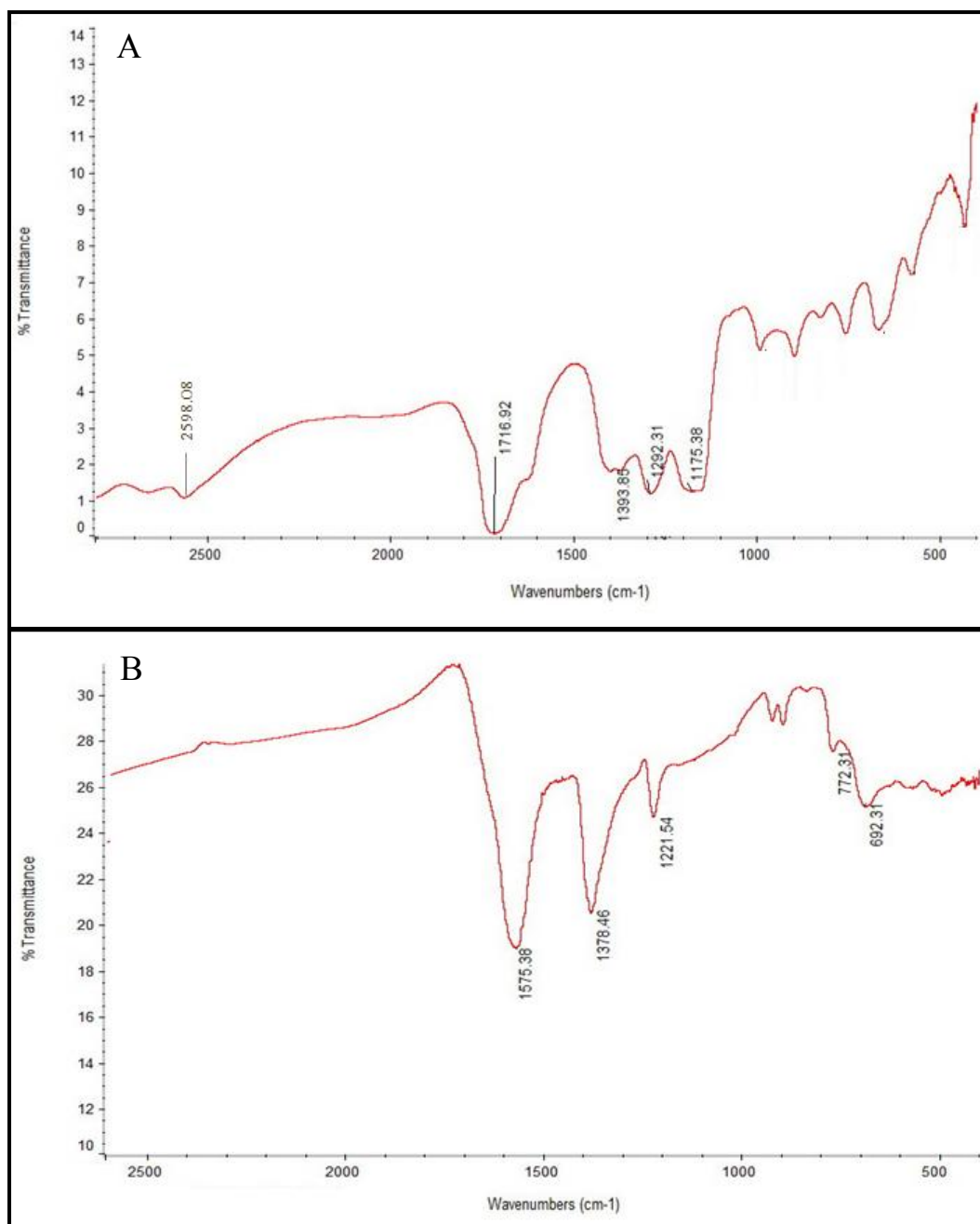


Figure 4.4 IR spectra of (A) TGA and (B) TGA-capped CdTe QDs

4.3 Fabrication of carbon nanotubes-modified screen-printed carbon electrodes (SPCNTEs)

4.3.1 Electrochemical behavior of SPCNTE and bare screen-printed carbon electrodes (SPCE)

In this research, the CNT electrodes were fabricated by mixing the functionalized CNTs with carbon ink, and the mixture was screen-printed on PVC substrates. These electrodes were chosen to be used here because they are inexpensive, flexible to design, easy to fabricate and suitable for electroanalytical techniques. The cyclic voltammetry (CV) was used to investigate the performance of the electron-transfer at the working electrodes. A bare SPCE was also used as the working electrode in the comparative study with the SPCNTE. The cyclic voltammograms of a solution containing TGA-capped CdTe QDs in PBS at bare SPCE (Figure 4.5, curve a) and SPCNTE (Figure 4.5, curve b) in the potential range of 0 to -1.8 V are shown in Figure 4.5. From Figure 4.5, the SPCNTE exhibited much higher current response compared to current at SPCE. These results indicated that CNTs eased the CdTe QDs reduction and decreased the potential barriers on the SPCEs. Therefore, SPCNTE was chosen as a novel working electrode for applying to an ECL sensor, which is based on the light emission arising from the electron-transfer reaction between electrochemiluminescence species.

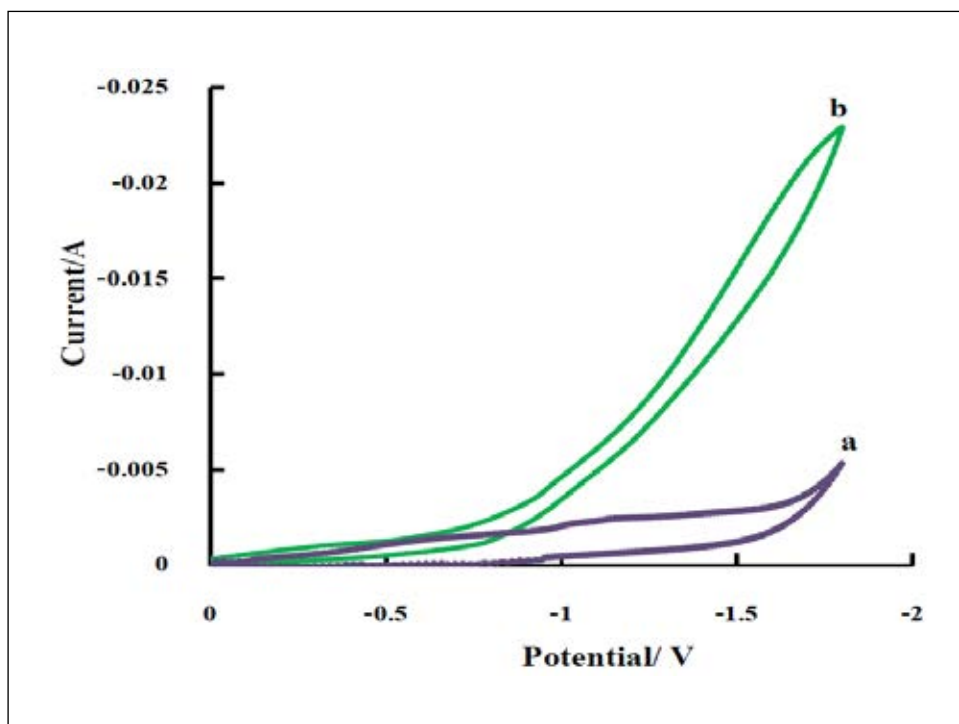


Figure 4.5 CV voltammograms of TGA-capped CdTe QDs at (a) bare SPCEs and at (b) SPCNTEs in 0.1 PBS (pH 8).

4.3.2 Electrochemiluminescence behavior of SPCNTE and SPCE

As shown Figure 4.6, the significant ECL behaviors of CdTe QDs at SPCNTEs (curves b) were observed. The ECL signal showed that SPCNTEs greatly facilitated the ECL of CdTe QDs. In contrast, it can be seen that the ECL intensity of CdTe QDs at bare SPCEs (curves a) was much lower than that observed at SPCNTEs. These phenomena are likely due to the fact that the effective surface area of the CNTs-modified electrode was much larger than that of the bare SPCEs. It can be explained that CNTs performed as nanowires connecting between CdTe QDs with electrode surface. These connections introduced many electrocatalytic sites onto the electrode surface and encouraged the electron transfer through the conducting tunnels of CNTs. Consequently, electron transfer in the ECL process at SPCNTEs was accelerated as compared with that at bare SPCEs, and the efficiency of producing excited-state QDs was enhanced.

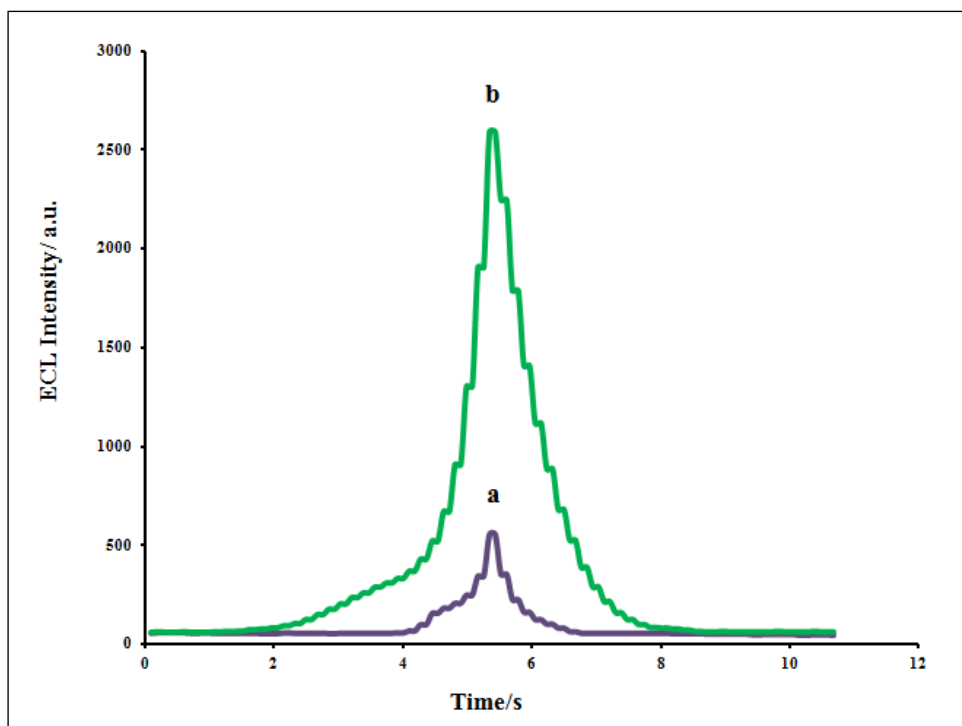


Figure 4.6 ECL-time curves of TGA-capped CdTe QDs at (a) bare SPCEs and at (b) SPCNTes in 0.1 M PBS (pH 8).

4.4 Electrochemiluminescence of CdTe quantum dots (CdTe QDs ECL) sensor based on the SPCNTes for determination of homocysteine (Hcy)

4.4.1 Effect of $K_2S_2O_8$ co-reactant

In ECL studies, there are two main mechanisms: one is ion annihilation ECL and the other is co-reactant ECL. Thus, we propose that potassium peroxydisulfate ($K_2S_2O_8$) can accelerate the radical species generation, acts as the co-reactant media in emission process, resulting in the amplification of the QDs ECL intensity. Upon a potential scan, the CdTe QDs is reduced to CdTe QD $^{\cdot-}$ species due to charge injection, while the co-reactant peroxydisulfate ion ($S_2O_8^{2-}$) is reduced to produce a strong oxidizing agent ($SO_4^{\cdot-}$), which quickly injects a hole into the valence band of reduced CdTe QDs species (CdTe QD $^{\cdot-}$) to produce the excited CdTe QDs (CdTe QD *), species that emit light in the aqueous solution. The possible ECL reaction mechanisms are described in Figure 4.7 and the following equations:

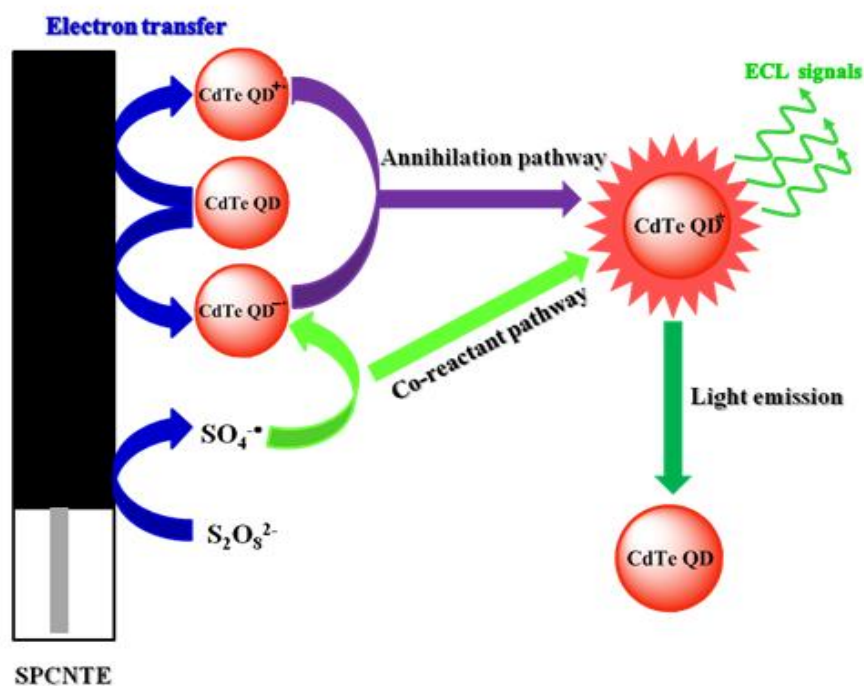
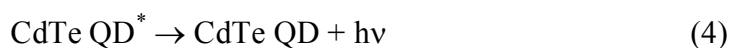
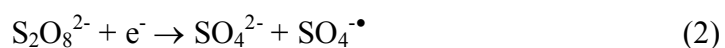


Figure 4.7 The mechanism of ECL of CdTe QDs on the SPCNTE.

Other than the ECL generated via an annihilation pathway between reduced and oxidized species as in Figure 4.7, there is another proposed pathway, namely ECL-2. The ECL-2 is attributed to the electron-transfer reaction between electrochemically reduced CdTe QD species ($\text{CdTe QD}^{\bullet-}$) and reduced co-reactant species ($\text{SO}_4^{\bullet-}$).

As theoretically predicted, the increased ECL intensity was observed when 0.005 M $S_2O_8^{2-}$ was added in the CdTe QD solution. The ECL spectra shown in Figure 4.8 indicate time-resolved ECL intensity from the solution of CdTe QDs and $S_2O_8^{2-}$, showing that the emission intensity increased upon the addition of $S_2O_8^{2-}$.

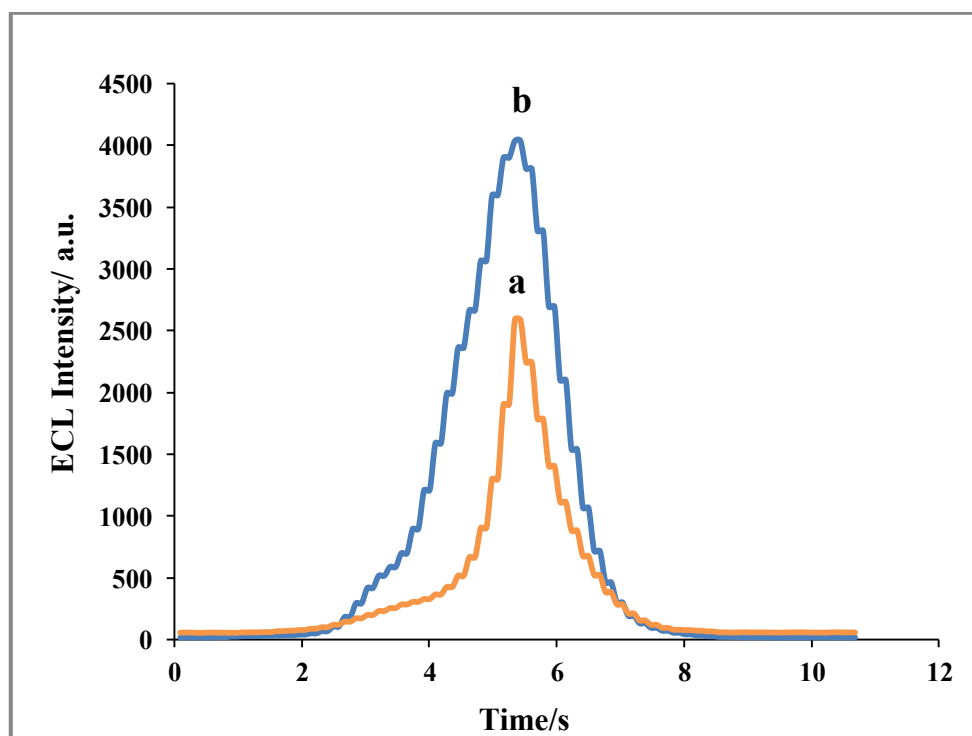
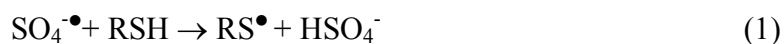


Figure 4.8 ECL-time curves of TGA-capped CdTe QDs at SPCNTEs in 0.1 M PBS (pH 8) (a) in the absence of $S_2O_8^{2-}$ and (b) in the presence of 0.005 M $S_2O_8^{2-}$.

4.4.2 Determination of homocysteine based on the quenching effect

The quenching effect of homocysteine on TGA-capped CdTe QDs ECL intensity at SPCNTEs was studied and shown in Figure 4.9. Upon the addition of 20 μM homocysteine to the PBS solution containing 5 μM CdTe QDs, the CdTe QDs ECL intensity decreased greatly. The relationship between ECL emission of TGA-capped CdTe QDs at SPCNTEs and homocysteine concentration revealed that the detection mechanism was based on the quenching effect of homocysteine with the following reaction:



The reason for quenching effect of homocysteine could be explained that a reactive sulfhydryl group (-SH) of homocysteine (RSH) react with dissolved oxygen, $\text{S}_2\text{O}_8^{2-}$ or their intermediate species produced in the processes of CdTe QDs ECL to form disulfide (RS-SR) and resulted in the lowering of ECL intensity. For this reason, the homocysteine concentration effect on the ECL intensity of CdTe QDs could be used for homocysteine quantification.

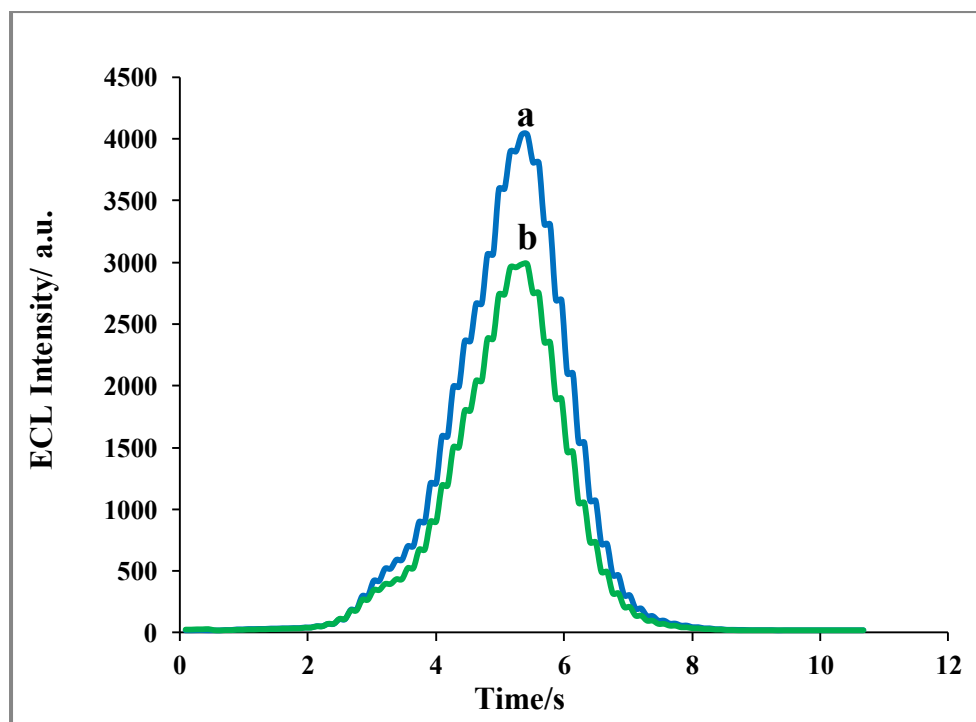


Figure 4.9 ECL-time curves of (a) TGA-capped CdTe QDs at SPCNTEs in 0.1 M PBS (pH 8) containing 0.005 M $K_2S_2O_8$ (b) in the presence of homocysteine at the concentration of 20 μ M.

4.5 Optimization of CdTe QDs ECL conditions

4.5.1 The effect of potential

The influence of the potential on the processes of CdTe QDs ECL was examined in the range of -1.0 to -1.6 V *vs.* Ag/AgCl. The results indicated that the intensity of the CdTe QDs ECL increased as the potential increased. Thus, a potential window of 0 to -1.6 V *vs.* Ag/AgCl was chosen for the highest CdTe QDs ECL intensity. The data for the effect of the potential are shown in Figure 4.10. However, if the potential was examined at condition above -1.6 V, the ECL detector could not detect the intensity due to the excess limitation of measurement.

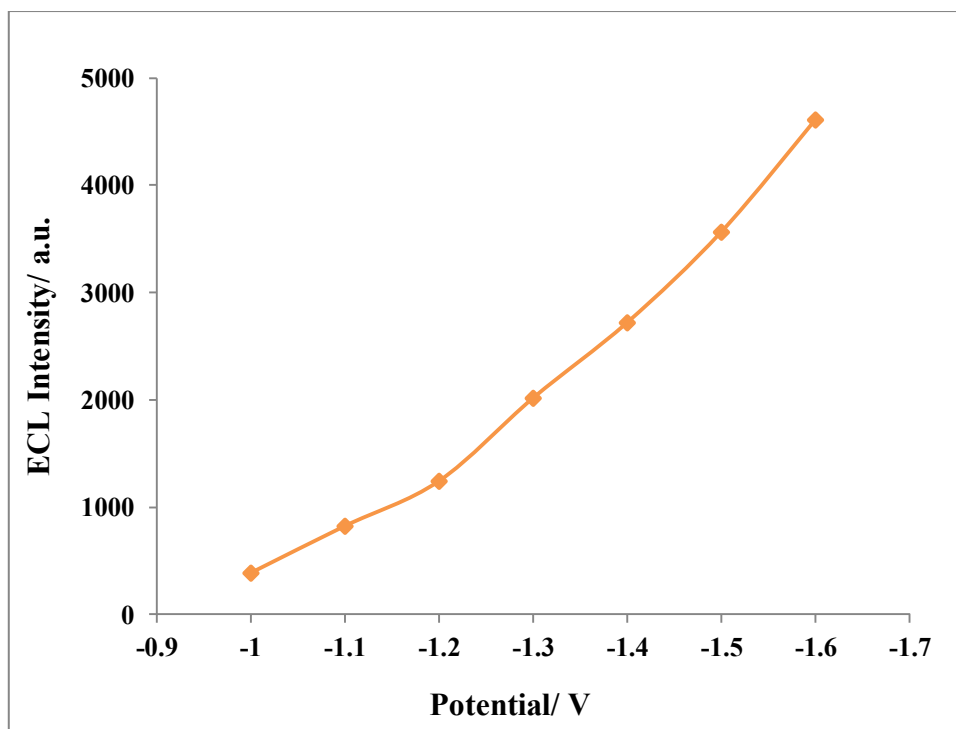


Figure 4.10 Effect of potential on CdTe QDs ECL (condition: scan rate, 0.15 V/s; step potential, 20 mV; the concentration of CdTe QDs, 5 μ M; 0.1 M PBS pH 8; SPCNTEs; PMT voltage, 800V).

4.5.2 The effect of scan rate

The effect of scan rate on the processes of CdTe QDs ECL at SPCNTEs was investigated in the range of 50 to 500 mVs^{-1} , and the results (see Figure 4.11) showed that a higher scan rate of the applied potential would cause a stronger CdTe QDs ECL intensity at SPCNTEs in the range of 50 to 150 mVs^{-1} . However, along with the increased scan rate above 150 mVs^{-1} , the increased scan rate induced decreasing in CdTe QDs ECL intensity. The explanation for this phenomena could be that the electrochemical process was irreversible, and high scan rate was unfavorable to electrochemical reaction of CdTe QDs. Therefore, 150 mVs^{-1} was chosen as the scanning rate for the maximum CdTe QDs ECL intensity.

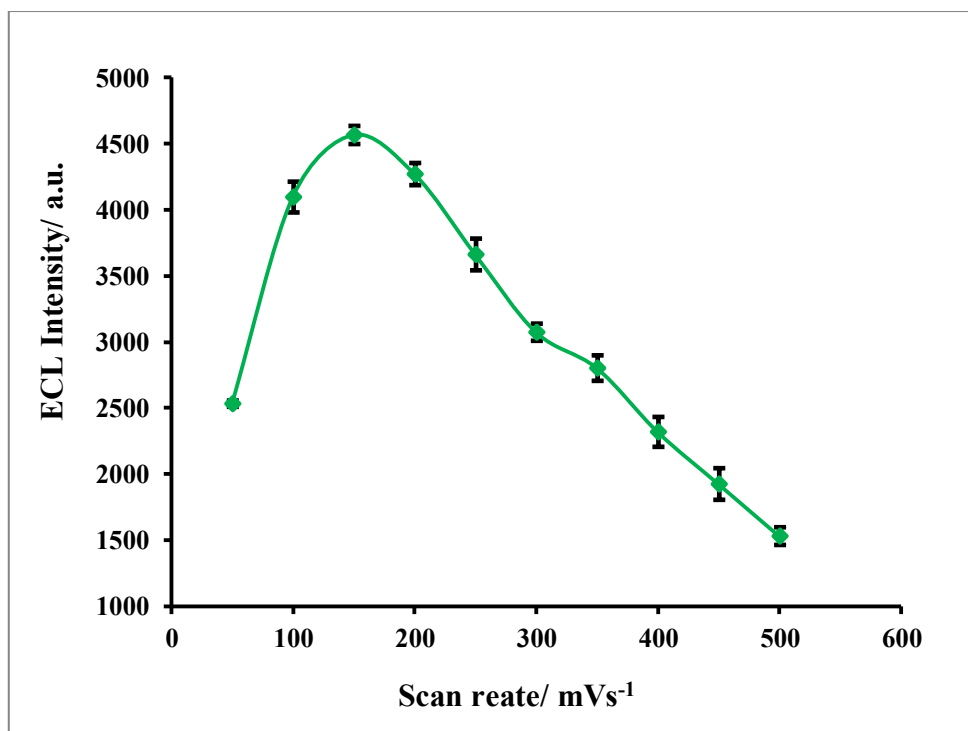


Figure 4.11 Effect of scan rate on CdTe QDs ECL (condition: potential window, 0 to -1.6 V; step potential, 20 mV; the concentration of CdTe QDs, 5 μ M; 0.1 M PBS pH 8; SPCNTEs; PMT voltage, 800V).

4.5.3 The effect of step potential

The effect of the step potential on the CdTe QDs ECL intensity was studied in the range of 15 to 40 mV, as shown in Figure 4.12. The results indicated that the intensity of the CdTe QDs ECL increased as the step potential increased in the range of 15 to 25 mV. Therefore, a step potential of 25 mV was selected for the highest CdTe QDs ECL intensity.

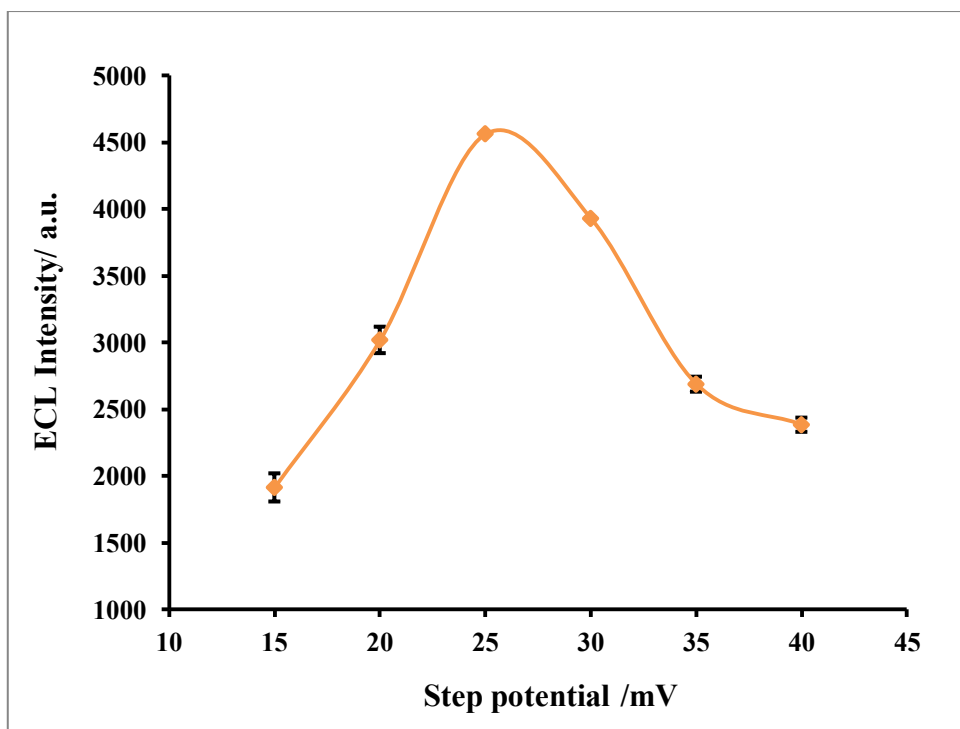


Figure 4.12 Effect of step potential on CdTe QDs ECL (condition: potential window, 0 to -1.6 V; scan rate, 0.15 V/s; the concentration of CdTe QDs, 5 μ M; 0.1 M PBS pH 8; SPCNTEs; PMT voltage, 800V).

4.5.4 The effect of concentration of CdTe QDs

The effect of concentration of CdTe QDs was studied at QDs concentration of 1, 3, 4, 5, 6, 7, 8, 10 and 11 μ M (see Figure 4.13). When the concentrations of CdTe QDs were increased, the reactive individual CdTe QD species in the electrochemical scanning process increased, resulting in the enhancement of ECL intensity. However, when the concentration of the CdTe QDs exceeded 6 μ M, the CdTe QDs ECL intensity decreased, indicating that the excessive CdTe QDs could inhibit the generation of excited-state CdTe QDs. The inhibition of generation of CdTe* is most likely due to an effect called self-absorption in higher concentration [51]. Therefore, 6 μ M of CdTe QDs was selected in order to obtain the highest ECL intensity in the assay.

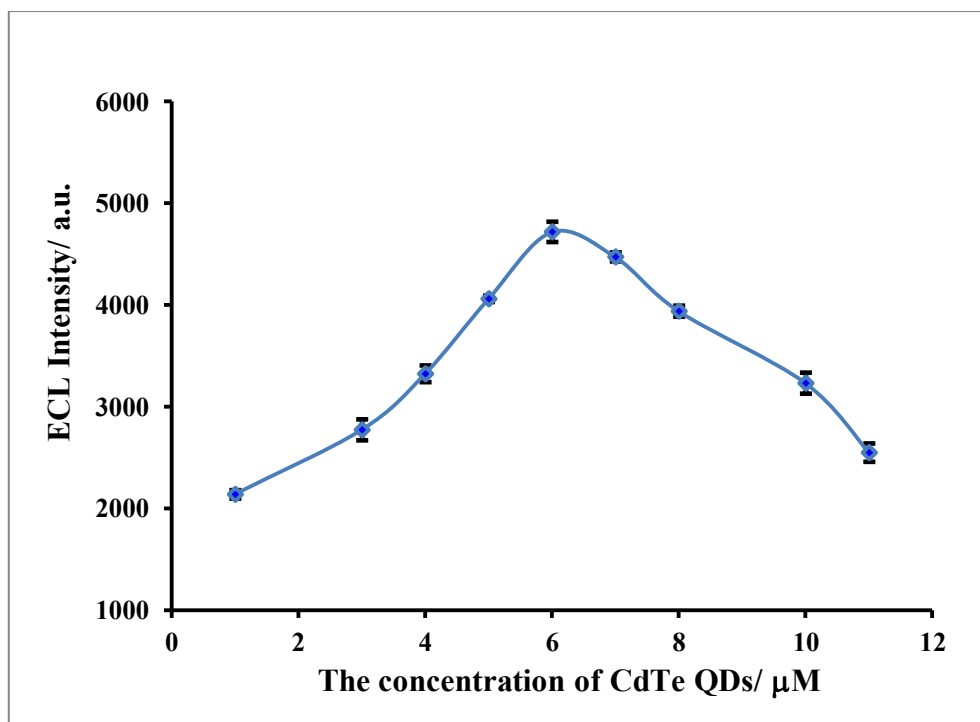


Figure 4.13 Effect of concentration of CdTe QDs (condition: potential window, 0 to - 1.6 V; scan rate, 0.15 V/s; step potential, 20 mV; 0.1 M PBS pH 8; SPCNTes; PMT voltage, 800V).

4.5.5 The effect of concentration of $\text{K}_2\text{S}_2\text{O}_8$ co-reactant

In this experiment, the effect of concentration of $\text{K}_2\text{S}_2\text{O}_8$ co-reactant on CdTe QDs ECL intensity was investigated at 0.5, 1, 5, 10, 15, 20, 25 and 30 mM of $\text{K}_2\text{S}_2\text{O}_8$. As shown in Figure 4.14, when the concentrations of $\text{K}_2\text{S}_2\text{O}_8$ co-reactant were increased, light emission intensity of CdTe QDs ECL increased dramatically, indicating that concentration of $\text{K}_2\text{S}_2\text{O}_8$ co-reactant was an important co-reactant for the production of CdTe QDs ECL in the solution. When the concentration of $\text{K}_2\text{S}_2\text{O}_8$ co-reactant exceeded 10 mM, the CdTe QDs ECL intensity decreased, indicating that the excessive $\text{K}_2\text{S}_2\text{O}_8$ co-reactant could inhibit the generation of excited-state CdTe QDs. It is likely that when $\text{K}_2\text{S}_2\text{O}_8$ is excessive, the reduced CdTe QDs species are not enough to react the excess $\text{K}_2\text{S}_2\text{O}_8$ co-reactant, causing the decrease in CdTe* species. For the reason mentioned above, 10 mM of concentration of $\text{K}_2\text{S}_2\text{O}_8$ co-reactant was selected in order to obtain the highest ECL intensity.

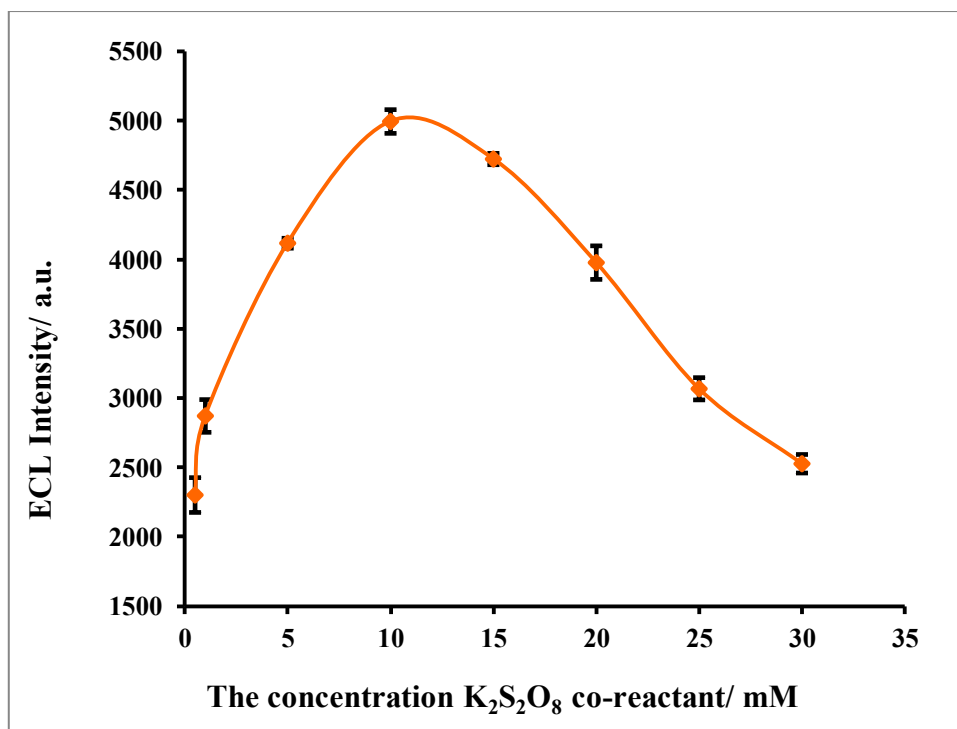


Figure 4.14 Effect of concentration of $K_2S_2O_8$ on CdTe QDs ECL (condition: potential window, 0 to -1.6 V; scan rate, 0.15 V/s; step potential, 20 mV; the concentration of CdTe QDs, 6 μ M; 0.1 M PBS pH 8; SPCNTes; PMT voltage, 800V).

4.5.6 The effect of pH of the PBS solution

The pH of the buffer solution is a significant factor influencing the CdTe QDs ECL reaction. Therefore, the effect of pH on the ECL signal was studied in the pH ranging from 5.0 to 10.0 prepared in PBS solutions. As shown in the Figure 4.15, it was found that the ECL intensity increased gently with the increasing pH. When the pH of buffer solutions became higher than 8, CdTe QDs ECL intensity began to decrease clearly. Thus, pH 8 was selected as an optimal pH value of PBS on the CdTe QDs ECL.

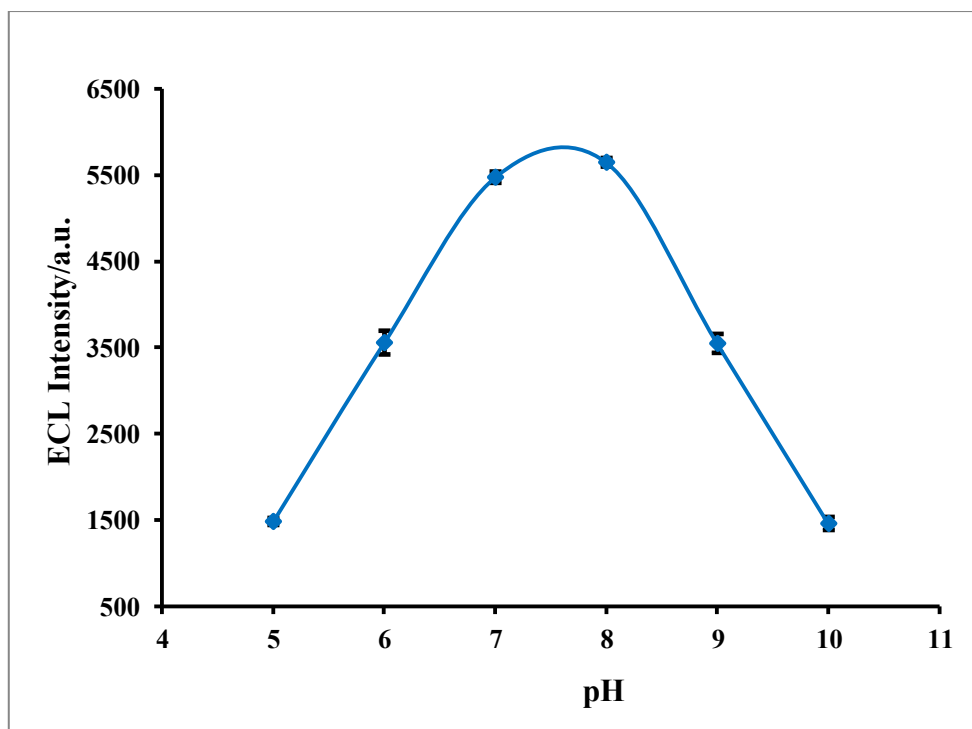


Figure 4.15 Effect of PBS pH on CdTe QDs ECL (condition: potential window, 0 to -1.6 V; scan rate, 0.15 V/s; step potential, 20 mV; the concentration of CdTe QDs, 6 μM ; SPCNTEs; PMT voltage, 800V).

4.6 Reproducibility and stability study

The reproducibility and stability of SPCNTEs were studied in ECL system of CdTe QDs. Each Hcy concentration at 5, 15 and 30 μM was performed using our proposed device under the optimal condition for 10 cycles of measurement. As shown in Figure 4.16, it was found that the SPCNTE was very stable and had excellent reproducibility for CdTe QDs ECL. The RSD for the 10 cycles of detection of 5, 15 and 30 μM Hcy is 0.53%, 1.07% and 1.18%, respectively. Thus, these results indicate that the SPCNTEs was an ideal working electrode for the studies of CdTe QD ECL.

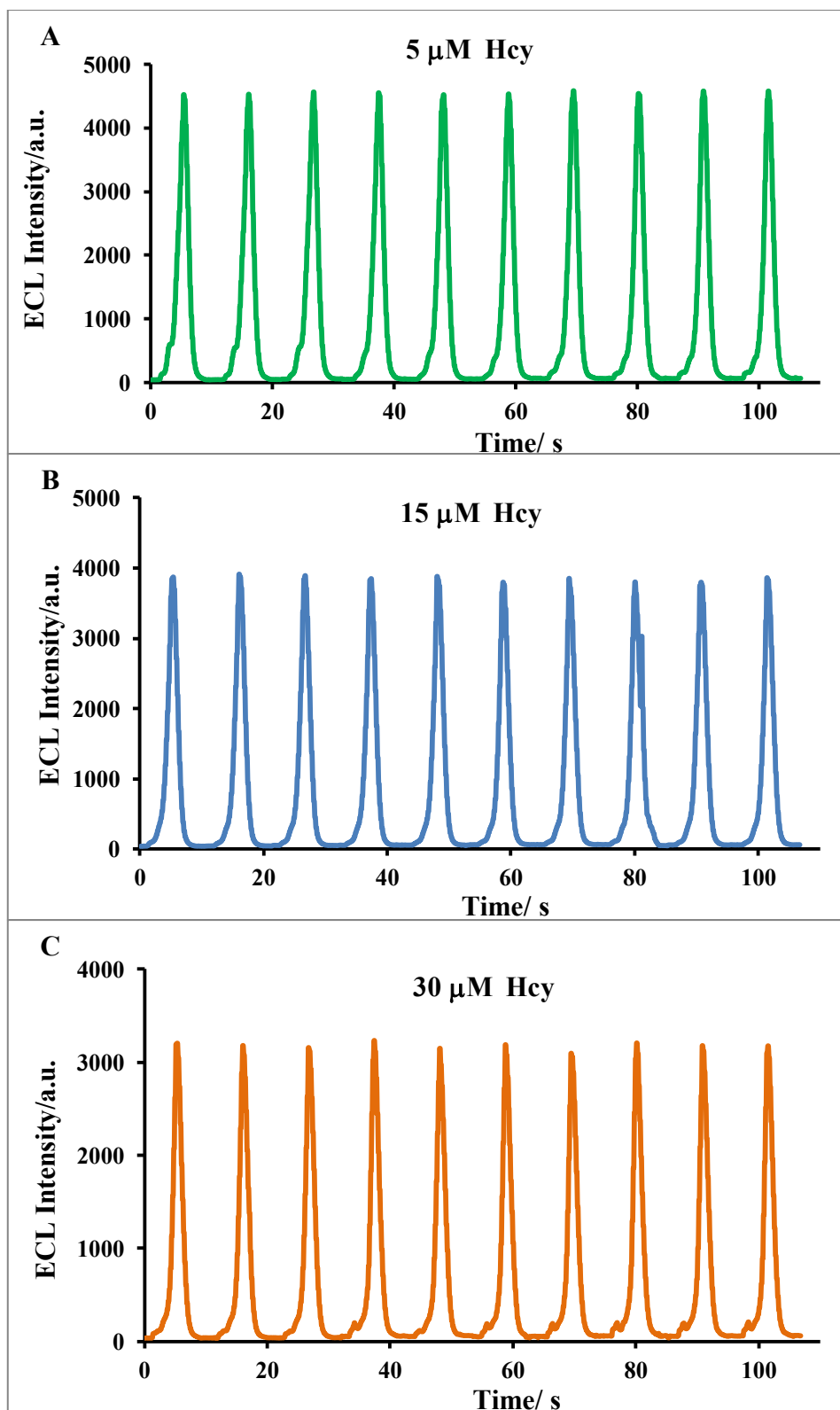


Figure 4.16 Reproducibility and stability of SPCNTEs (condition: potential window, 0 to -1.6 V; scan rate, 0.15 V/s; step potential, 25 mV; the concentration of Hcy, (A) 5 μM (B) 15 μM (C) 30 μM; SPCNTEs; PMT voltage, 800V).

4.7 The analytical performance

4.7.1 Linearity

The analytical performance of Hcy was investigated under the optimal condition. The calibration curve was obtained by the quenching effect of Hcy on the CdTe QDs ECL intensity. As shown in Figure 4.17, the quenching effect of various concentration of Hcy on the CdTe QDs ECL intensity was studied. Obviously, the CdTe QDs ECL intensity decreases with the increase in Hcy concentration. From the Figure 4.18, the calibration range for the determination of Hcy was employed by plotting $\ln(I_0/I)$ against the concentration of Hcy, where I_0 and I are the ECL intensities in absence and presence of Hcy, respectively. The curve has a linear range from 5 to 35 μM with a coefficient (r^2) of 0.9971.

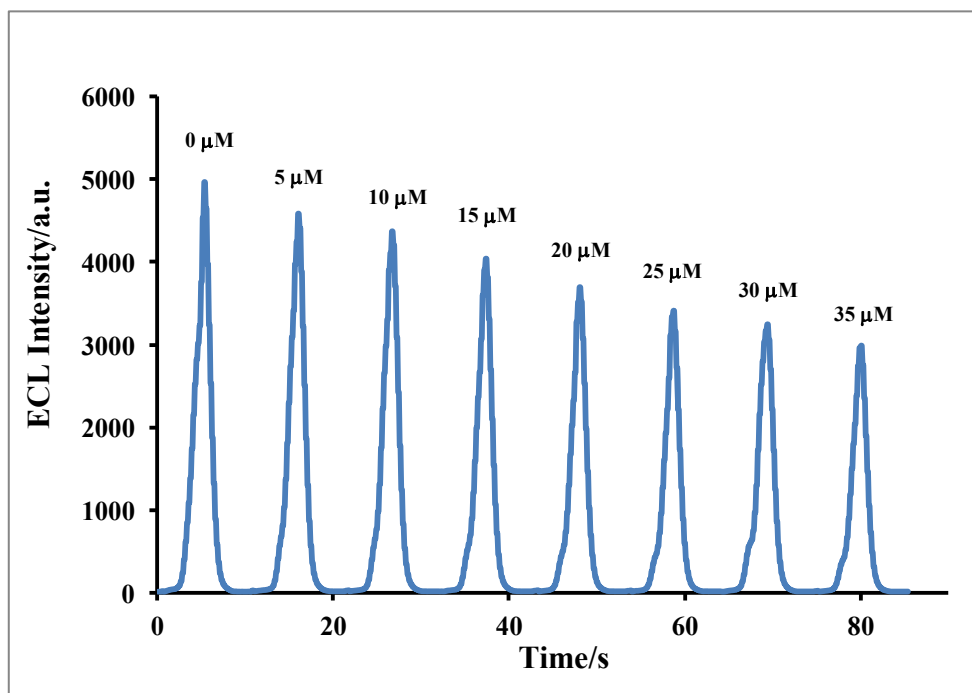


Figure 4.17 ECL-time curves of TGA-capped CdTe QDs at SPCNTEs in 0.1 M PBS (pH 8) containing 10 mM $\text{K}_2\text{S}_2\text{O}_8$ in the presence of homocysteine at the concentration of 5, 10, 15, 20, 25, 30 and 35 μM .

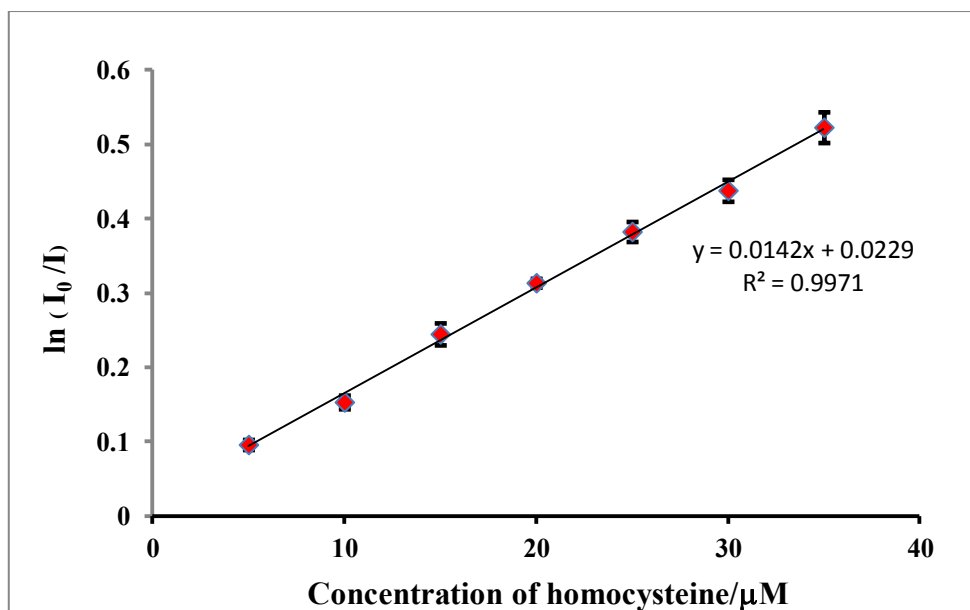


Figure 4.18 Calibration curve for determination of Hcy (condition: potential window, 0 to -1.6 V; scan rate, 0.15 V/s; step potential, 25 mV; the concentration of CdTe QDs, 6 μM ; SPCNTEs; PMT voltage, 800V).

4.7.2 Limit of detection (LOD) and Limit of quantification (LOQ)

The limit of detection (LOD) and limit of quantification (LOQ) were used to describe the smallest concentration of the analyte that can be reliably measured using our proposed device on CdTe QDs ECL system. LOD was determined using statistical method from the calibration curve in the range of 5 to 35 μM and calculated from $3S_{\text{blank}}$ and LOQ was determined statistical method from the calibration curve in the range of 5 to 35 μM and calculated from $10S_{\text{blank}}$, where S_{blank} is the standard deviation of blank measurement ($n = 3$). The LOD and LOQ of Hcy were found to be 0.011 μM and 0.037 μM , respectively.

4.8 Interference effect

To study the effect of the interference for the determination of Hcy, two related amino thiols, which are cysteine and glutathione. The 20 μM Hcy solutions with different concentrations of each interference were used for CdTe QDs ECL measurements under the optimal condition. Interference was defined as when a negative or positive change of 10% or more was observed compared to the response recovery of Hcy alone (see Table 4.1).

As shown in Figure 4.19, the effect of cysteine for the detection of Hcy was that 20 to 400 μM of cysteine concentration did not affect the detection of Hcy. However, cysteine was able to affect the detection of Hcy when the concentration of cysteine was higher than 400 μM . Thus, this method could be investigated for the detection of Hcy in real sample when the level of cysteine was lower than 400 μM .

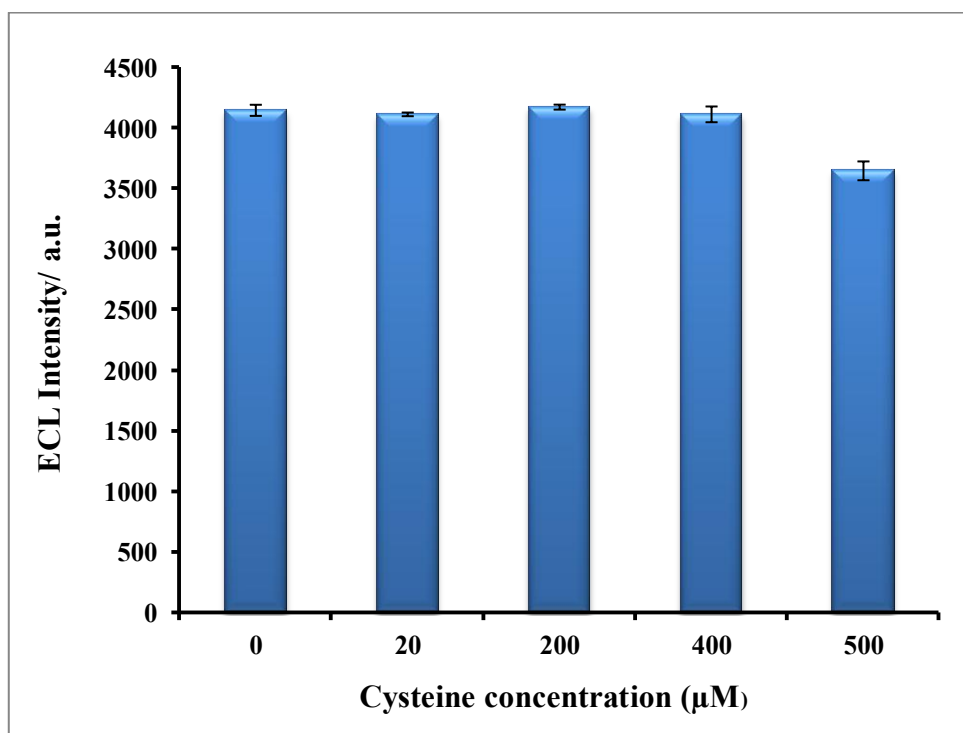


Figure 4.19 The effect of cysteine on the detection of Hcy.

From the Figure 4.20, the effect of glutathione for the detection of Hcy was shown. It was found that there was no effect of glutathione when the concentration of glutathione was in the range from 20 to 500 μM . When the concentration of glutathione was above 500 μM , it interfered with the detection of Hcy. Therefore, this method could be performed for the detection of Hcy in the presence of glutathione of less than 500 μM .

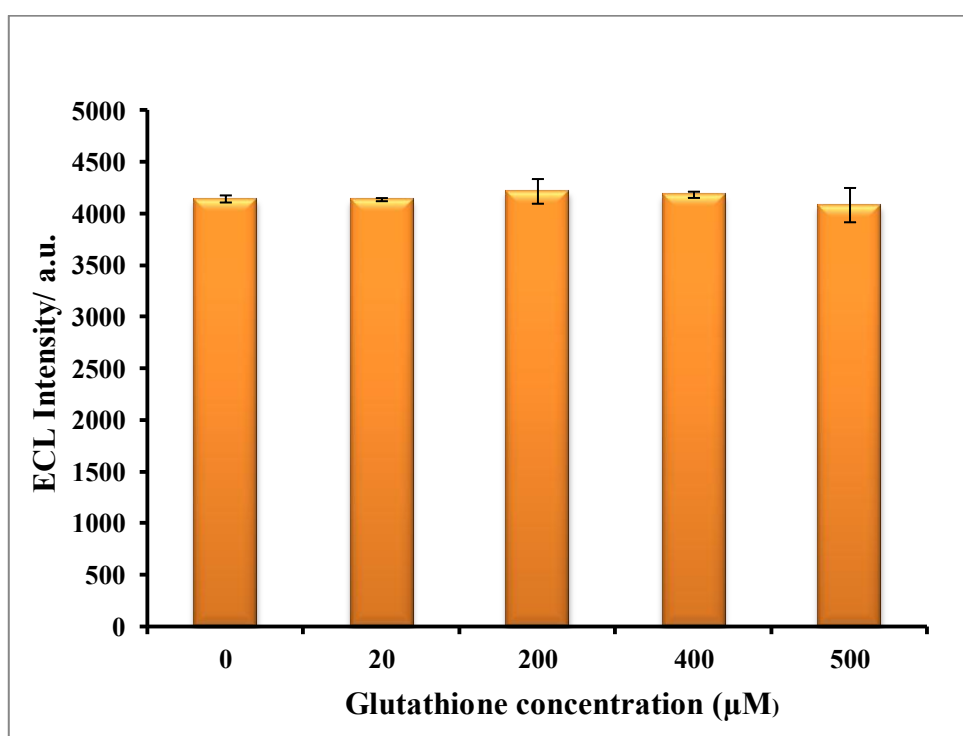


Figure 4.20 The effect of glutathione on the detection of Hcy.

Table 4.1 Effect of interfering on the detection of Hcy

Interferences	Concentration ratio of Homocysteine: interference	Recovery of Homocysteine signal (%)
Cysteine	1:1	99.19
	1:10	100.64
	1:20	99.20
	1:25	87.95
Glutathione	1:1	99.84
	1:10	101.77
	1:20	100.97
	1:25	98.56

4.9 Real sample analysis

The CdTe QDs ECL method in this research was applied to detect the concentrations of homocysteine in human urine and artificial urine. The standard addition method was used to investigating reliability and accuracy of the developed method. Each sample type was spiked with 5, 15 and 30 μM of Hcy. The spiked sample was prepared in triplicate and analyzed in triplicate runs.

Having evaluated the potential application of this method with pure single analyte solutions, the proposed method was evaluated using a real biological sample, that is, in the presence of other potentially interfering components. The unknown concentration of Hcy in urine was determined using this TGA-capped CdTe QDs ECL procedure based on the SPCNTEs. The results were listed in Table 4.2. The Hcy standard solution was added into the urine and the recovery efficiencies of both urine samples were obtained in the range of 95.93-100.67%, which are acceptable under all conditions. In addition, the %RSD were below 2% that the proposed method showed the %RSD value less than the AOAC International recommended value.

Table 4.2 The results of Hcy determinations in human urine sample and artificial urine sample by CdTe QDs ECL.

Samples	Spiked level (μM)	Found (μM)	Recovery (%)	RSD (%)
Human urine	0.00	N.D.		
	5.00	4.84 ± 0.06	96.89	1.16
	15.00	14.39 ± 0.11	95.93	0.79
	30.00	29.59 ± 0.05	98.65	0.18
Artificial urine	0.00	N.D.		
	5.00	4.92 ± 0.06	98.4	1.27
	15.00	14.85 ± 0.07	98.98	0.45
	30.00	29.02 ± 0.06	100.67	0.49

N.D. = not detected

CHAPTER V

CONCLUSIONS

5.1 Conclusions

In this work, TGA-capped CdTe QDs ECL procedure based on the SPCNTEs was successfully developed and applied for the determination of Hcy levels in urine samples for the first time. The synthesized TGA-capped CdTe QDs used in ECL procedure based on the SPCNTEs were characterized by UV–Vis spectroscopy, PL spectroscopy, TEM and IR spectroscopy. From the characterizations, the average size of TGA-capped CdTe QDs was approximately 2.53 nm, which considered close to the diameter of 2.47 nm resulting from the calculations using UV-Vis absorption spectra of the QDs. The concentration of as-synthesized TGA-CdTe QDs is 7.39×10^{-3} M.

The SPCNTEs were fabricated by mixing the functionalized CNTs with carbon ink and screen-printing on PVC substrates. It was found that the SPCNTEs exhibited much higher current response compared to current at SPCEs. Thus, the SPCNTEs could greatly enhance ECL intensity of TGA-CdTe QDs, decrease their ECL onset potential and ECL peak potential, which avoiding the interferences resulted from high potential in TGA-capped CdTe QDs solution.

Furthermore, a novel approach for the determination of homocysteine was developed based on the quenching effect of homocysteine in the TGA-CdTe QDs ECL sensor. A prerequisite for good analytical performance was the use of the sample pH 8 at the conditions: potential window, 0 to -1.6 V; scan rate, 0.15 V/s; step potential, 25 mV; the concentration of TGA-CdTe QDs, 6 μ M; concentration of $K_2S_2O_8$, 10 mM; SPCNTEs; PMT voltage, 800V. Under the optimal condition, the Hcy concentration was in linearity with $\ln(I_0/I)$ in the range of 5 to 35 μ M. The detection limit of 0.011 μ M of this proposed method is lower than the conventional method and limit of quantification (LOQ) was found to be 0.037 μ M. The precision expressed as RSD were in the range of 0.53 to 1.18% for 10 replicates at three

concentration levels (5, 15 and 30 μM) of Hcy. Before studying the potential applications in real sample, the effects of interference were investigated. This proposed method could be carried out for the determination of homocysteine when the level of cysteine and glutathione did not exceed 400 μM and 500 μM , respectively. Moreover, this TGA-capped CdTe QDs ECL procedure based on the SPCNTEs was applied to detect homocysteine level in real samples of human urine and artificial urine. The unknown concentration of homocysteine in human urine and artificial urine were detected using this TGA-capped CdTe QDs ECL procedure based on the SPCNTEs and the recovery of spiked Hcy was in a range of 95.93-100.67%. Therefore, the proposed method provides simple, inexpensive, excellent sensitive, reproducible and fast analysis for Hcy.

5.2 Future perspective

In the future, this TGA-capped CdTe QDs ECL procedure based on the SPCNTEs has a potential to be applied for the determination of other thiol compounds in human and it can be developed for a simultaneous determination of multiple thiol compounds such as, homocysteine, cysteine and glutathione.

REFERENCES

- [1] Su, L.X., and Li, Y. Quantum dot biolabeling coupled with immunomagnetic separation for detection of *Escherichia coli* O157:H7. Analytical Chemistry 76 (2004): 4806-4810.
- [2] Lu, Q., Moore, J. M., Huang, G., Mount, A. S., Rao, A. M., Larcom, L. L., and Ke, P. C. RNA polymer translocation with single-walled carbon nanotubes. Nano Letters 4 (2004): 2473-2477.
- [3] Smith, A. M., and Nie, S. Semiconductor nanocrystals: structure, properties, and band gap engineering. Accounts of Chemical Research 43 (2010): 190-200.
- [4] Yin, Y. D., and Alivisatos, A. P. Colloidal nanocrystal synthesis and the organic-inorganic interface. Nature 437 (2005): 664-670.
- [5] Alivisatos, A. P. Semiconductor clusters, nanocrystals, and quantum dots. Science 271 (1996): 933-937.
- [6] Burda, C., Chen, X., Narayanan, R., and El-Sayed, M. A. The chemistry and properties of nanocrystals of different shapes. Chemical Reviews 105, (4) (2005): 1025-1102.
- [7] Richter, M. Electrochemiluminescence (ECL). Chemical Reviews 104 (2004): 3003-3036.
- [8] Pyati, R. and Richter, M. M. ECL--Electrochemical luminescence. Annual Reports on the Progress of Chemistry, Section C: Physical Chemistry 103 (2007): 12-78.
- [9] Forster, R. J., Bertocello, P., and Keyes, T. E. Electrogenerated chemiluminescence. Annual Review of Analytical Chemistry 2 (2009): 359-385.
- [10] Rivera, V. R., Gamez, F. J., Keener, W. K., and Poli, M. A. Rapid detection of *Clostridium botulinum* toxins A, B, E, and F in clinical samples, selected food matrices, and buffer using paramagnetic bead-based electrochemiluminescence detection. Analytical Biochemistry 353 (2006): 248-256.

- [11] Chi, Y., Duan, J., Lin, S., and Chen, G. Flow injection analysis system equipped with a newly designed electrochemiluminescent detector and its application for detection of 2-thiouracil. Analytical Chemistry 78 (2006): 1568-1573.
- [12] Wang, J., Yang, Z., Wang, X., and Yang, N. Capillary electrophoresis with gold nanoparticles enhanced electrochemiluminescence for the detection of roxithromycin. Talanta 76 (2008): 85-90.
- [13] Ding, Z., Quinn, B. M., Haram, S. K., Pell, L. E., Korgel, B. A., and Bard, A. J. Electrochemistry and electrogenerated chemiluminescence from silicon nanocrystal quantum dots. Science 296 (2002): 1293-1297.
- [14] Lin, Z. Y., Sun, J. J., Chen, J. H., Guo, L., and Chen, G. N. Electrochemistry Communication 9 (2007): 269.
- [15] Chu, X., Duan, D. X., Shen, G. L., and Yu, R. Q., Amperometric glucose biosensor based on electrodeposition of platinum nanoparticles onto covalently immobilized carbon nanotube electrode. Talanta 71 (2007): 2040-2047.
- [16] Lin, Z. Y., Chen, J. H., and Chen, G. N. An ECL biosensor for glucose based on carbon-nanotube/Nafion film modified glass carbon electrode. Electrochimica Acta 53 (2008): 2396-2401.
- [17] Gaponik, N., Gaponik, D. V., Rogach, A. L., Hoppe, K., Shevchenko, E. V., Kowski, A., Eychmüller, A., and Weller, H. Thiol-capping of CdTe nanocrystals: An alternative to organometallic synthetic routes. The Journal of Physical Chemistry B 106 (2002): 7177-7185.
- [18] Chuanuwatanakul, S., Dungchai, W., Chailapakul, O., and Motomizu, S. Determination of trace heavy metals by sequential injection-anodic stripping voltammetry using bismuth film screen-printed carbon electrode. Analytical Sciences 24 (2008): 589-594.
- [19] Kuznetsova, A., Mawhinney, D. B., Naumenko, V., Yates Jr, J. T., Liu, J., and Smalley, R. E. Enhancement of adsorption inside of single-walled

- nanotubes: opening the entry ports. Chemical Physics Letter 321 (2000): 292–296.
- [20] Yu, W., Qu, L. H., Guo, W. Z., and Peng, X. G. Experimental determination of the extinction coefficient of CdTe, CdSe, and CdS nanocrystals. Chemistry of Materials 15 (2003): 2854-2860.
- [21] Murray, C. B., Norris, D. J., and Bawendi, M. G. Synthesis and characterization of nearly monodisperse CdE (E = sulfur, selenium, tellurium) semiconductor nanocrystallites. Journal of the American Chemical Society 115 (1993): 1 8706–8715.
- [22] Hines, A. M., and Sionnest, G. P. Bright UV-blue luminescent colloidal ZnSe nanocrystals. The Journal of Physical Chemistry B 102 (1998): 3655–3657.
- [23] Kohn, S. E., Yu, P. Y., Petroff, Y., Shen, Y. R., Tsang, Y., and Cohen, M. L. Electronic band structure and optical properties of PbTe, PbSe, and PbS. Physical Review B 10 (1974): 3720.
- [24] Micic, I. O., Curtis, J. C., Jones, M. K., Sprague, R. J., and Nozik, J. A. Synthesis and characterization of InP quantum dots. The Journal of Physical Chemistry, 98 (1994): 4966–4969.
- [25] A quantum paintbox. Chemistry World [online]. Available from: <http://www.rsc.org/chemistryworld/Issues/2003/September/paintbox.asp> [2012, September 13].
- [26] Pinwattana, K., Wang, J., Lin, T. C., Wu, H., Du, D., Lin, Y., and Chailapakul, O. CdSe/ZnS quantum dots based electrochemical immunoassay for the detection of phosphorylated bovine serum albumin. Biosensors and Bioelectronics 26 (2010): 1109–1113.
- [27] Asgari, M., Shanehsaz, M., Shamsipur, M., Behzad, M., and Maragheh, G. M. Electrochemical reduction of dioxygen on a thioglycolic acid-capped CdTe quantum dots modified glassy carbon electrode. Journal of Applied Electrochemistry 43 (2013): 15-19.

- [28] Liu, X., Jiang, H., Lei, J., and Ju, H. Anodic electrochemiluminescence of CdTe quantum dots and its energy transfer for detection of catechol derivatives. Analytical Chemistry 79 (2007): 8055–8060.
- [29] Liu, X., and Ju, H. Coreactant enhanced anodic electrochemiluminescence of CdTe quantum dots at low potential for sensitive biosensing amplified by enzymatic cycle. Analytical Chemistry 80 (2008): 5377–5382.
- [31] Jiang, H., and Ju, H. Electrochemiluminescence sensors for scavengers of hydroxyl radical based on its annihilation in CdSe quantum dots film/peroxide system. Analytical Chemistry 79 (2007): 6690–6696.
- [32] Rubinstein, I., and Bard, J. Electrogenerated chemiluminescence. 37. Aqueous Ecl systems based on $\text{Ru}(2,2'\text{-bipyridine})_3^{2+}$ and oxalate or organic acid. Journal of the American Chemical Society 103 (1981): 512-516.
- [33] Carbon Nanotubes - Polymer Nanocomposites [online]. (n.d.). Available from: <http://www.intechopen.com/books/carbon-nanotubes-polymer-nanocomposites> [2012, September 13].
- [34] Catalytic Synthesis of Carbon Nanotubes [online]. (n.d.). Available from: <http://cobweb.ecn.purdue.edu/~catalyst/Carbon%20Nanotubes/Catalytic%20Nanotubes/Catalytic%20Synthesis%20of%20Carbon%20Nanotubes.htm> [2008, March 24].
- [35] Silaste, M. L. Dietary effects on antioxidants, oxidised LDL and homocysteine [online]. 2003. Available from: <http://herkules.oulu.fi/isbn9514270703/html/x305.html> [2012, September 13].
- [36] Lochman, P., Adam, T., Friedecký, D., Hlídková, E., and Skopková, Z. High-throughput capillary electrophoretic method for determination of total aminothiols in plasma and urine. Electrophoresis 24 (2003): 1200–1207.
- [37] Refsum, H., Smith, D. A., Ueland, M. P., Nexø, E., Clarke, R., McPartlin, J., Johnston, C., Engbaek, F., Schneede, J., McPartlin, C., and Scott, M. J. Facts and recommendations about total homocysteine

- determinations: An expert opinion. Clinical Chemistry 50 (2004): 3–32.
- [38] Frick, B., Schröcksnadel, K., Neurautera, G., Wirleitner, B., Artner-Dworzak, E., and Fuchs, D. Rapid measurement of total plasma homocysteine by HPLC. Clinica Chimica Acta 331 (2003): 19-23.
- [39] Lawrence, N. S., Deo, R. P., and Wang, J. Detection of homocysteine at carbon nanotube paste electrodes. Talanta 63 (2004): 443–449.
- [40] Chwatko, G., and Jakubowski, H. The determination of homocysteine – thiolactone in human plasma. Analytical Biochemistry 337 (2005): 271-277.
- [41] Zhang, D., Zhang, M., Liu, Z., Yu, M., Li, F., Yi, T., and Huang, C. Highly selective colorimetric sensor for cysteine and homocysteine based on azo derivatives. Tetrahedron Letters 47 (2006): 7093-7096.
- [42] Agüí, L., Farfal, P. C., Sedeño, Y. P., and Pingarrón, M. J. Electrochemical determination of homocysteine at a gold nanoparticle-modified electrode. Talanta 74 (2007): 412–420.
- [43] Lin, H. J., Chang, W. C., and Tseng, L. W. Fluorescent sensing of homocysteine in urine: using fluorosurfactant-capped gold nanoparticles and o-Phthaldialdehyde. Analyst 135 (2010): 104–110.
- [44] Leesutthiphonchai, W., Dungchai, W., Siangproh, W., Ngamrojnavanichd, N., and Chailapakul, O. Selective determination of homocysteine levels in human plasma using a silver nanoparticle-based colorimetric assay. Talanta 85 (2011): 870-876.
- [45] Choi, N. H., Lee, Y. J., Lyu, K. U., and Lee, Y. W. Tris(2,2'-bipyridyl)ruthenium(II) electrogenerated chemiluminescence sensor based on carbon nanotube dispersed in sol-gel-derived titania-Nafion composite films. Analytica Chimica Acta 565 (2006): 48–55.
- [46] Huang, R., Zheng, X., and Qu, Y. Highly selective electrogenerated chemiluminescence (ECL) for sulfide ion determination at multi-

- wall carbon nanotubes-modified graphite electrode. Analytica Chimica Acta 582 (2007): 267–274.
- [47] Lina, Z., Chena, J., and Chen, G. An ECL biosensor for glucose based on carbon-nanotube/Nafion film modified glass carbon electrode. Electrochimica Acta 53 (2008): 2396–2401.
- [48] Hua, L., Han, H., and Chen, H. Enhanced electrochemiluminescence of CdTe quantum dots with carbon nanotube film and its sensing of methimazole. Electrochimica Acta 54 (2009): 1389–1394.
- [49] Jang, S. K., Ko, C. H., Moon, B., and Lee, H. Observation of photoluminescence in polypyrrole micelles. Synthetic Metals 150 (2005): 127–131.

APPENDICES

APPENDIX A

Table A1 The intensity of ECL signal from CdTe QDs and added Hcy in the human urine sample

Added Hcy (mM)	Intensity			ln(I ₀ /I)				
	1	2	3	1	2	3	Average	SD
0	4820.0	4826.6	4828.0	-	-	-	-	-
5	4590.1	4585.4	4579.8	0.0489	0.0511	0.0490	0.0496	0.0012
15	3695.2	3683.0	3693.4	0.2657	0.2703	0.2658	0.2673	0.0026
30	2610.1	2614.0	2604.0	0.6134	0.6131	0.6153	0.6139	0.0012

Table A2 The intensity of ECL signal from CdTe QDs and added Hcy in the artificial urine sample

Added Hcy (mM)	Intensity			ln(I ₀ /I)				
	1	2	3	1	2	3	Average	SD
0	4916.0	4932.0	4966.0	-	-	-	-	-
5	4697.0	4705.0	4699.0	0.0456	0.0471	0.0553	0.0464	0.0052
15	3817.0	3800.0	3806.0	0.2530	0.2607	0.2660	0.1516	0.0065
30	2789.0	2753.0	2778.0	0.5668	0.5830	0.5809	0.4159	0.0088

APPENDIX B

Precision and accuracy

Table B1 Accuracy considered from AOAC manual for peer verified methods program, VA, NOV 1993.

Analyte concentration	Mean % recovery
100%	98-102
10%	98-102
1%	97-103
0.1%	95-105
100 ppm	90-107
10 ppm	80-110
1 ppm	80-110
100 ppb	80-110
10 ppb	60-115
1 ppb	40-120

Table B2 Precision considered from AOAC manual for peer verified methods program, VA, NOV 1993.

Analyte concentration	%RSD
100%	± 1.3
10%	± 2.7
1%	± 2.8
0.1%	± 3.7
100 ppm	± 5.3
10 ppm	± 7.3
1 ppm	± 11
100 ppb	± 15
10 ppb	± 21
1 ppb	± 30

VITA

NAME : Miss Triyaporn Kittisarakul
ADDRESS : 145 Pasijaroen Road, Amphoe Muang,
 Ubon Ratchathani 34000, Thailand
E-MAIL : orkly_twinhell@hotmail.com

PERSONAL INFORMATION

Date of Birth : April 4, 1987
Nationality : Thai

EDUCATION

2003-2006 : Major of Science-Mathematic, Benchama Maharat School
 2006-2010 : Bachelor Degree of Science Program in Chemistry, Srinakharinwirot
 University
 2010-2012 : Master Degree of Science Program in Chemistry, Chulalongkorn
 University

Poster Presentation:

2012	Sokendai Asian Winter School 2012 “Frontiers in Photo-Molecular Science”, Okazaki, Japan
2013	Pure and Applied Chemistry International Conference (PACCON 2013), Chon Buri, Thailand.
2013	The 4 th CU-UM-NUS Trilateral Meeting Symposium, Bangkok, Thailand

Proceeding:

Triyaporn Kittisarakul, Numpon Insin, Orawon Chailapakul, Suchada Chuanuwatanakul “Electrogenerated chemiluminescence of CdTe quantum dots capped with thioglycolic acid for determination of thiol compounds” Proceedings of Pure and Applied Chemistry International Conference (PACCON 2013), The Tide Resort, Chon Buri, Thailand, January 23-25, 2013, pp 93-97.